

A LIQUID TIN DISPENSER ARC CATHODE

including a new method to separate the anode fall  
from the cathode fall.

A thesis submitted by DONALD JAMES DICKSON for the  
Ph.D. Degree in the faculty of science of the  
University of London.

Applied Electron Physics,  
Imperial College of Science and  
Technology, London, S.W.7.

October 1966

ABSTRACT.

This thesis describes an arc cathode of the 'cold' or 'vapour' type which has advantages over the usual liquid or solid types. Liquid metal (tin) is supplied at a slow rate through a porous conducting substrate; the result is a cathode having the dimensional stability of a solid and the 'self-healing' properties of a liquid.

It is verified that the usual techniques of estimating the cathode and anode falls of potential are unsatisfactory. The difficulties involved in probe measurements are investigated.

A new method is described for measuring the cathode fall and anode fall of an arc discharge separately - this represents a distinct advance in arc technique as previous attempts have always measured their sum. The method is tested on other cathodes besides tin, and it has proved possible to study the electrode falls of the carbon arc in air when it changes from the thermionic to the vapour mode on reducing the ambient pressure.

This method also permits the measurement of the variation of potential with distance immediately in front of the cathode, with a resolution approaching  $10^{-6}$  cm. This too is a new achievement since other techniques, such as probes, are not readily applicable owing to the high current densities and temperatures prevailing.

Finally, the future prospects of the tin dispenser cathode and the new measurement techniques are discussed.

ACKNOWLEDGMENTS.

This work was supervised by Professor D. Gabor, F.R.S. to whom I am grateful for suggesting the tin dispenser cathode. It is a pleasure to acknowledge his interest throughout this research programme.

I am indebted to Dr. A. von Engel of the Clarendon Laboratory, Oxford, for many valuable suggestions and discussion.

For assistance in the design and construction of experimental apparatus Mr. P. Robinson and Mr. L. Borroff deserve thanks.

For suggestions and discussion I thank Drs. D. Jones and J.R.Cozens, and my other colleagues in the Applied Electron Physics Laboratory.

Finally, the Science Research Council, without whose financial support this work could not have been done, I thank for the award of a Research Studentship.



ELECTRIC ARC

1mm

(Details: cooled copper anode above plane tin dispenser cathode, 80% oxygen + 20% argon at a total pressure of 760 torr. Current 10 amperes)

CONTENTS.

<u>CHAPTER I. THE ARC DISCHARGE.</u>	<u>Page</u>
1.1. Introduction	7
1.2. Historical	7
1.3. The positive column	9
1.4. The electrodes	10
1.5. Estimating the electrode falls	12
1.6. Cold (or vapour) arc cathodes	13
1.7. The mechanism of the cold cathode arc	14
1.8. Liquid and solid cold cathodes	20
1.9. The aim of the present research	21
 <u>CHAPTER II. APPARATUS.</u>	
2.1. Simple arc tube	22
2.2. Demountable vacuum system	22
2.3. Further modifications	26
 <u>CHAPTER III. DESIGN OF A TIN DISPENSER CATHODE.</u>	
3.1. Tin pool cathode and anchoring experiments	29
3.2. Wick cathodes	31
3.3. Porous discs	33
3.4. Mounting the porous discs	34
3.5. Behaviour of the tin dispenser cathode	37
3.6. Electrical characteristics	38
 <u>CHAPTER IV. PROBE MEASUREMENTS.</u>	
4.1. Purpose	41
4.2. General theory of probe measurements	43
4.3. Previous probe measurements on arcs at high pressure	45
4.4. Flying probe measurements	47

	<u>Page</u>
4.5. Rotating probe	49
4.6. Probe theory at high pressures	51
4.7. Discussion of probe results	57
4.8. Conclusions	59

CHAPTER V. SEPARATE MEASUREMENTS OF THE CATHODE FALL  
AND ANODE FALL.

5.1. Introduction	60
5.2. Principle of the method	61
5.3. Experimental details	62
5.4. Measurement of the anode velocity	67
5.5. Results with a tin cathode	69
5.5.1. Cathode fall measurement	69
5.5.2. Influence of anode material	73
5.5.3. Current dependence	74
5.5.4. Influence of ambient gas	74
5.5.5. Pressure dependence	79
5.5.6. Conclusion	80
5.6. Results with a graphite cathode	80
5.6.1. Introduction	80
5.6.2. The graphite arc in argon	83
5.6.3. The graphite arc in air	85
5.6.4. Summary of carbon arc measurements	86
5.7. Results with other electrode materials	88
5.7.1. Copper	88
5.7.2. Tungsten	89
5.8. Discussion of measurements of $V_c$ and $V_a$	90

CHAPTER VI. THICKNESS OF THE CATHODE REGION.

6.1. Definition of the cathode region	95
6.2. Method	96
6.3. The cathode region thickness of the tin arc	96
6.4. Current dependence	97
6.5. Influence of ambient gas pressure	97
6.6. Interpretation of oscillograms at low pressure	101
6.7. Thickness of the cathode fall sheath	102
6.8. Discussion of Results	103

CHAPTER VII. FLUCTUATIONS.

7.1. Introduction	108
7.2. Experimental Results	108
7.3. Discussion	110

CHAPTER VIII. CONCLUSIONS.

8.1. The tin dispenser cathode	111
8.2. A new method of separating the anode fall from the cathode fall	112
8.3. The thickness of the fall sheaths	112
8.4. Suggestions for future work	113

<u>REFERENCES.</u>	114
--------------------	-----

## CHAPTER 1. THE ARC DISCHARGE.

### 1.1. Introduction.

The passage of electricity through a gas, usually known as a 'discharge', may take a number of forms which are self-sustaining once initiated. When a circuit carrying several amperes is broken by separating a pair of electrodes, the gap will be bridged by a cylinder of luminous gas; this is known as an electric arc. Bright spots on the electrodes show where the current passes between the solid (or liquid) electrodes and the gas. The major part of the arc, known as the 'arc column' or 'positive column', is influenced by winds and convection currents so that its appearance depends on the ambient gas pressure and also on the orientation of the electrodes. If the electrodes are in a horizontal plane, the convection currents cause the discharge to rise in the gap to higher than the electrode plane to give a characteristic arc shape, from which the discharge was named.

### 1.2. Historical.

The electric arc was discovered at the beginning of the nineteenth century, the earliest studies being probably made by Petroff<sup>1</sup> (1803) and Davy<sup>2</sup> (1812), but the first detailed work was carried out by Hertha Ayrton<sup>3</sup> (1902) on the carbon arc in air. This was followed by investigations covering a wide range of electrode materials, gases and pressures<sup>4</sup>. In much of the early work, the arc was too short for a fully-developed positive column



to be obtained and the complex relationships between the arc parameters arise from the dominating influence of the electrodes. Grotrian<sup>5</sup> obtained arcs up to 50 cm long by stabilising the column in the centre of a glass tube by means of a spiral air flow, and found a linear relationship between arc voltage and arc length.

The nature of the charge carriers was investigated by Mitkewicz<sup>6</sup> (1903) who decided they were mainly electrons moving towards the anode. The source of the electrons was supposed to be the hot spot on the cathode, by thermionic emission.<sup>6,7</sup>

The high temperature of the electric arc was apparent by the ease with which substances could be melted thereby; this led rapidly to its use as a source of illumination and in chemical reactions. The temperature in the positive column has been measured by a number of methods. Suits<sup>8</sup> (1935), by determining the velocity of sound in the column found gas temperatures in the range 4,000-6,000°K. A variety of methods used by other workers have given similar results. Engel and Steenbeck<sup>9</sup> measured the gas density (which gives the temperature) from the absorption of X-rays. Edels<sup>10</sup> has obtained temperatures from measurements of shock velocities. The temperature can also be measured spectroscopically.

At the electrodes, the arc terminates in spots where the current density is much higher than in the column. Estimates of the current density in the cathode spot have increased with improvements in technique from 10 amperes/cm<sup>2</sup> (Stark, 1904, mercury cathode)<sup>7</sup> to 10<sup>6</sup> amperes/cm<sup>2</sup> (Froome, 1949, mercury cathode)<sup>11</sup>. This high

current density, in addition to the rapid random motion of many arc cathode spots, makes cathode studies rather difficult and there is still doubt as to the mechanism of certain types of arc.

### 1.3. The Positive Column.

The mechanism of the positive column is fairly well understood. Electrons travel from cathode to anode under the influence of the electric field due to the voltage applied to the electrodes. To maintain the quasi-neutrality of the column, an equal density of positive ions must be present which, owing to their larger mass and opposite charge, move slower than the electrons towards the cathode. Since solids do not normally emit ions, the ions are assumed to be produced in the body of the discharge by collisions between sufficiently energetic electrons and gas atoms or molecules. Charged particles may be lost to the walls of the containing vessel by diffusion, owing to the radial concentration gradient, but the charge concentrations are normally such that the slower ions 'hold back' the faster electrons electrostatically; the resulting diffusion coefficient is much closer to the ion diffusion coefficient than to that for electrons and the process is known as 'ambipolar' diffusion.

Provided the gas pressure is above about 30 torr, the ions, electrons and gas atoms are in thermal equilibrium owing to the large number of collisions.

The voltage gradient along the arc column may be estimated by measuring arc voltage as a function of arc length, or by vibrating one

of the electrodes along the arc axis<sup>12</sup>. The result, at atmospheric pressure, is usually in the range 10-100 volt/cm depending on the ambient gas and also on the electrode material, owing to evaporation. Suits<sup>12</sup> found that the voltage gradient was independent of the arc length for arcs longer than about 3 mm.

#### 1.4. The Electrodes.

In the solid, the current is carried wholly by electrons and in the gas by electrons and ions; the transition takes place in the electrode spots. Also a sharp temperature change of several thousand degrees takes place at the gas-solid interface.

Owing to their respective potentials, the cathode will attract positive ions and repel electrons whereas the anode will repel positive ions and collect electrons. The result is a tendency for an excess of positive ions to be present close to the cathode, and for an excess of electrons close to the anode surface. This produces an electric field, which could be obtained from Poisson's equation  $\frac{dX}{dx} = 4\pi\rho$ , where  $X$  is the field and  $\rho$  the charge density, if the charge distribution were known. For a steady state, the rate of removal of both signs of charges must be the same, and since the electrons have a much higher mobility than the positive ions, this is achieved by a much higher field at the cathode than at the anode. These regions of high field are known as the cathode fall and anode fall respectively, fig.1. The cathode fall is usually of the order of the ionisation potential of a gas component, say 10

(1) Charge carriers and their behaviour:

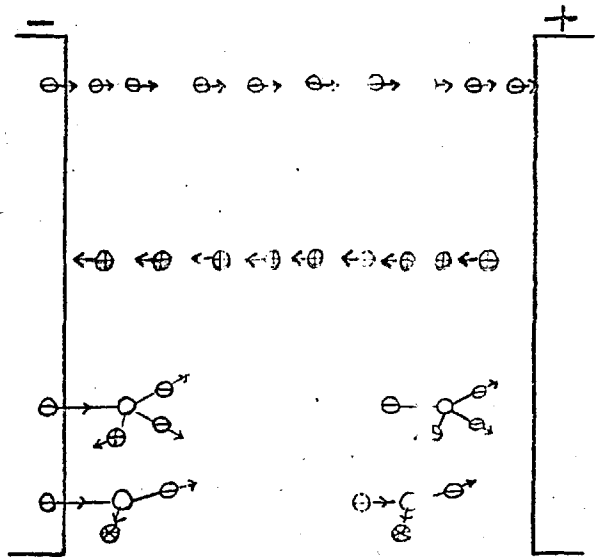
⊖ electron, ⊕ positive ion, ○ neutral atom, ⊗ excited atom.

electrons emitted from cathode travel to anode under influence of the applied field

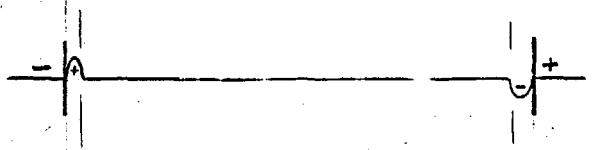
ions produced between the electrodes (by collisions) travel towards cathode, but move slower than the electrons

ionisation

excitation



(2) Space charge distribution:



(3) Potential distribution (schematic)

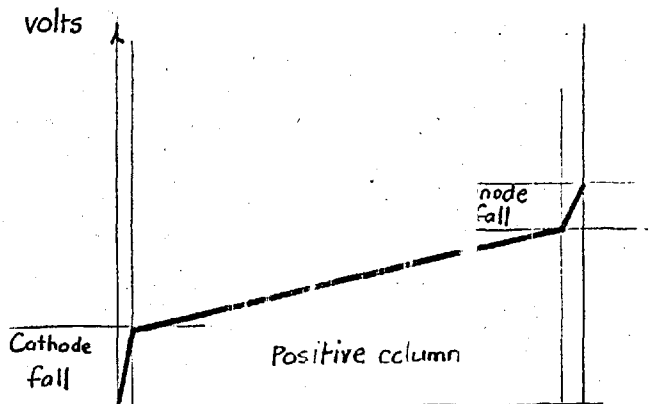


Fig 1. The electric arc.

volts, and its thickness is generally believed to be of the order  $10^{-6}$  cm<sup>13</sup> so that the field is of the order  $10^7$  volt/cm.

It is convenient, at this stage, to divide arc cathodes into two classes; those in which the observed cathode current densities can be accounted for by thermionic emission (carbon, tungsten) and those metals of lower melting point which vapourise appreciably at temperatures too low for sufficient thermionic emission. The first class can be considered reasonably well understood, but not the others, which are usually known as 'cold' or 'vapour' arcs and, at one time or another, as many mechanisms have been suggested as there are ways of extracting electrons from metals. It seems surprising that the cathode fall for the two types is almost the same.

Measurements of temperature and current density in the cold cathode spot are seldom better than order of magnitude estimates. Temperature measurement by pyrometry is liable to be frustrated by dense vapour close to the cold cathode surface.

#### 1.5. Estimating the Electrode Falls.

If the arc voltage is plotted against arc length, with the current constant, a near straight line results if the arc is not too short, which can be extrapolated back to zero arc length. Where this line cuts the voltage axis may be expected to give an estimate of the sum of the anode and cathode falls. This method, however, will probably give an answer which is too large since it includes

the contribution of the contracted regions of the column close to the electrodes.

Alternatively, if the arc is shortened by moving the electrodes towards each other, until they touch, it is found that the arc voltage decreases slowly at first, and then drops abruptly to zero at contact, from a value which gives an estimate of the sum of the electrode falls<sup>14</sup>.

Both these methods give the anode fall + cathode fall, and in the past these have been approximately separated by using different combinations of anode and cathode material.

#### 1.6. Cold or Vapour Arc Cathodes.

The behaviour of an arc cathode spot on a cold cathode is different from a thermionic one. For example, on a carbon cathode (thermionic) the cathode spot is a stationary region of white-hot carbon with a current density of about 500 amperes/cm<sup>2</sup>,<sup>14</sup> whereas on a typical cold cathode the cathode spot is much smaller and more mobile, the current density being about 10<sup>6</sup> amperes/cm<sup>2</sup>. The loss of cathode material from the cold cathode is considerable.

There is no necessity for the cathode to be solid, in fact, liquid mercury cathodes have been used for many years in high current rectifiers. In addition to the low voltage drop across the mercury arc, there is the additional advantage that the system can be accidentally overloaded without permanent damage to the cathode surface. The mercury cathode is one of the best examples

of the inadequacy of the thermionic theory since the boiling point of mercury is  $357^{\circ}\text{C}$ . The main disadvantage of mercury is the spray of mercury droplets thrown up from the cathode surface which can cause trouble ('back-firing') if it lands on the anode. This can, to a certain extent, be cured by a technique known as 'anchoring'; if a piece of wetted metal (e.g. molybdenum) projects through the pool surface, the random motion of the cathode spot ceases and it becomes attached in the form of a line to the meniscus at the anchor.

Under suitable conditions, high boiling point materials such as tungsten and carbon, which 'normally' behave thermionically, support cold cathode spots.

#### 1.7. The Mechanism of the Cold Cathode.

This is the main problem associated with the cold cathode arc, stated simply: How can current densities of up to  $10^6$  amperes/cm<sup>2</sup> be extracted from a relatively cool metal surface, at the price of only 10 volts?

As pointed out above, thermionic emission can be reasonably discounted as a possibility owing to the low cathode temperature. While the source of electrons has been attributed to: thermal ionisation in front of the cathode,<sup>15,16</sup> 'hot' conduction electrons in the metal,<sup>17</sup> and thermal emission from 'conduction bands' in a dense vapour layer,<sup>18</sup> it is generally believed that the electrons arise either from field emission or due to the impact of excited atoms.

Field Emission Theory.

The emission of electrons due to lowering and deforming of the potential barrier at a cathode surface by means of a strong electric field is well known<sup>19</sup>. That the cold arc cathode could be explained by field emission was first suggested by Langmuir<sup>20</sup>. The strong field at the cathode surface is supposed to arise from the positive ion space charge there.

Mackeown<sup>21</sup> found an expression for the field  $E_c$  (volts/cm) at the cathode surface from Poisson's equation, in terms of electron and ion current densities,  $j_-$  and  $j_+$  (amperes/cm<sup>2</sup>) respectively, and the cathode fall  $V_c$  (volts).  $V_c$  was assumed to occur within one mean free path so that  $j_-$  and  $j_+$  are constant in the cathode fall thickness, and all ions reaching the cathode were absorbed.

He obtained:

$$E_c^2 = 7.57 \times 10^5 (V_c)^{\frac{1}{2}} (j_+ M^{\frac{1}{2}} / m^{\frac{1}{2}} - j_-) \quad \text{volt}^2 / \text{cm}^2$$

where  $M$  and  $m$  are the ion and electron masses respectively.

The electron current density drawn from a surface of work function  $\phi$  volts by a field of  $E$  volts/cm is given by the Fowler-Nordheim equation<sup>22</sup>:

$$j_- = 6.2 \times 10^{-6} \frac{(\mu/\phi)^{\frac{1}{2}}}{\mu + \phi} E^2 \exp\left(-6.8 \times 10^7 \frac{\phi^{3/2}}{E}\right) \quad \text{amp/cm}^2$$

where  $\mu$  is the Fermi energy in electron volts.

The implications of these two relations can be seen from fig.2 where the Mackeown equation is plotted for various values of  $j_-/j_+$



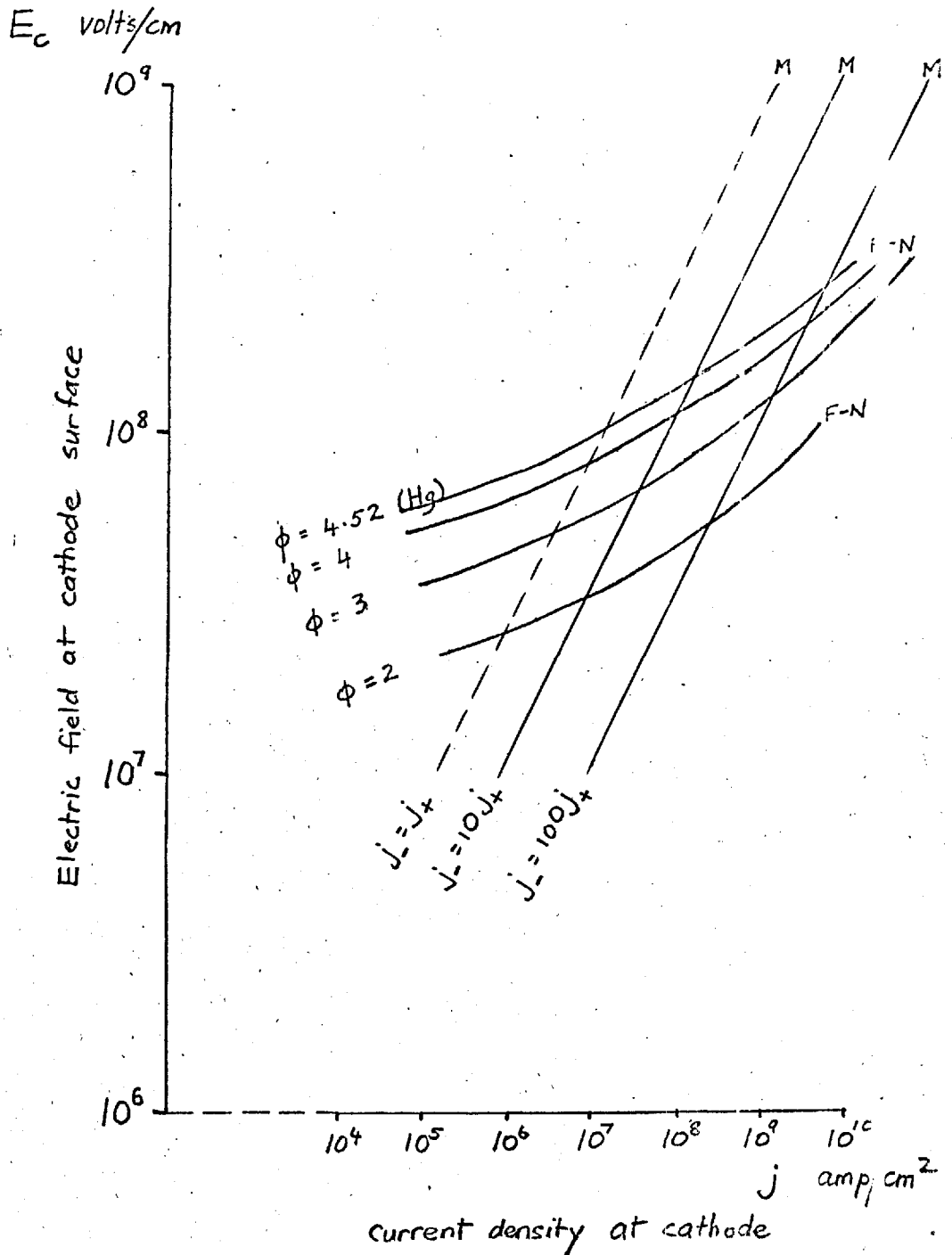


Fig 2. Simultaneous solution of Mackeown (M) and Fowler-Nordheim (F-N) equations assuming

$$(M/m)^{\frac{1}{2}} = 600 \quad \text{and} \quad V_c = 10 \text{ volts.}$$

and the Fowler-Nordheim equation for different work functions, assuming  $V_c = 10$  volts,  $M/m = 600^2$ . It is seen that even for surfaces of low work function ( $\phi = 2$ ) fields greater than  $10^7$  volts/cm are necessary to obtain any current at all, and that in order to produce such fields the cathode current density must be greater than  $10^6$  amperes/cm. The current density in the mercury cathode spot has been measured by Froome<sup>11</sup> as  $10^6$  amperes/cm<sup>2</sup>, but it seen from fig.2 that with a work function of  $\phi = 4.52$  volts, a current density of  $10^7$  to  $10^9$  amperes/cm<sup>2</sup> (depending on  $j_-/j_+$ ) is required to satisfy both equations. It is conceivable that the work function might be lowered by oxide layers or surface irregularities, but since emission occurs from a clean mercury pool, this seems unlikely to produce the large effect required. It should be pointed out, however, that rejection of the field theory hinges on the measured value of current density in the cathode spot, and it is a fact that estimates of the current density have increased with improvements in techniques; it may be that the current density is even higher than Froome's value. This is assumed by Hull<sup>23</sup> who uses the value  $10^7$  amp/cm<sup>2</sup>. The value of  $j_-/j_+$  also influences the field to be expected at a particular current density. This has not been measured directly, and is usually estimated from a consideration of the energy lost and gained at the cathode surface; most estimates are in the range 10 to 100.<sup>13</sup>

A further possibility has been suggested by Gabor<sup>24</sup> arising from some results obtained in experiments on thermionic conversion;

if ions were reflected from the cathode surface with a probability  $R$ , then at a given  $j_+$  the field would be increased as if the ion current were  $(1+R)/(1-R)$  times larger.

#### The Excitation Theory.

It has been suggested by von Engel and Robson<sup>13</sup> that electrons are released from the cold arc cathode by the impact of excited atoms.

It has been shown theoretically<sup>25</sup> and experimentally<sup>26</sup> that excited atoms can release electrons from a surface, with a yield of 0.1 to 1 electrons per incident atom, provided that the ionisation potential exceeds the work function.

The observed high current density at the arc cathode spot requires a high density of excited atoms to produce it; this high vapour density is maintained by back-scattering of evaporated atoms by incoming positive ions accelerated in the cathode fall. The majority of these back-scattered atoms are assumed to be in excited states, as a result of electron-atom collisions. Since a large proportion of the atoms leaving the cathode are returned to it, the experimentally measured net evaporation rate, from which cathode spot temperatures are usually calculated, is a small fraction of the atoms actually evaporated from the cathode surface; the estimated spot temperature is thus too low. von Engel and Robson estimate the cathode spot temperature  $T_c$  to be  $800^\circ\text{K}$  for a mercury cathode (compared with  $T_c = 350^\circ\text{C}$  from the net evaporation rate) corresponding to a saturated vapour pressure of about 10 atmospheres and a mean free path of vapour atoms less

than  $5 \times 10^{-7}$  cm, so that if the cathode fall thickness is of order  $10^{-6}$  cm, the assumption of many collisions and consequent back-scattering of evaporated atoms is justified.

Electrons emitted from the cathode are accelerated in the cathode fall space until they have sufficient energy to excite atoms ( $\text{Hg}^* = 4.9$  eV;  $\text{Sn}^* = 4.33$  eV). The electron will continue to move away from the cathode and the excited atom will emit a quantum of resonance light which can be absorbed by an unexcited atom, thus exciting it, and so on until the resonance radiation reaches the cathode surface whereupon an electron will be liberated (with a finite probability). It is shown that owing to the reflecting properties of the dense vapour region close to the cathode, most of the resonance radiation is reflected towards the cathode surface. Ions, necessary to produce the cathode fall, supply energy for evaporation and for back-scattering, can be produced by an electron collision with an excited atom or possibly by collisions between excited atoms, so that it is not necessary for the cathode fall to be greater than the ionisation potential. The cathode fall is greater than the first excitation potential of the appropriate species since, on the average, each electron must produce more than one excited atom.

If the vapour atoms have excited states of lower energy than the cathode work function, then these will not be capable of releasing electrons. This represents an additional loss of energy, and will result in a higher value of the cathode fall than the ionisation potential might suggest.

1.8. Liquid and Solid Cold Cathodes.

As was indicated above, a wide range of metals in the liquid or solid state can be used as arc cathodes. Liquid metal cathodes possess the advantage that any erosion or "fracture" of the cathode surface caused by the action of the cathode spot is immediately made good by the influx of cathode material from other parts of the cathode. The ejection of liquid droplets, and the consideration that it may be inconvenient in some applications to use a liquid (e.g. if the orientation of the device is variable) has led, from time to time, to attempts to combine the advantages of the liquid arc cathode with the dimensional stability and the engineering advantages of a solid.

One possible solution is to supply the cathode surface with liquid metal by some sort of wick, so that the arc is supplied with cathode material at the rate at which it is lost. 'Wick cathodes' on this principle are described in patents of Tonks<sup>27</sup> and also Steenbeck and Berthold<sup>28</sup>; these consisted of a refractory metal sintered sponge with mercury supplied either by capillary action from a pool in which the wick stood, or by means of pumping mercury through the porous sponge. Apparently the success of these devices was rather limited, as no evidence of practical application has been found.

1.9. The Aim of the Present Research.

This thesis is concerned with a 'wick cathode' capable of operating at higher operating temperatures than a mercury cathode, and in ambient gases at around atmospheric pressure. Tin has been chosen as the liquid metal, as its low melting point ( $232^{\circ}\text{C}$ ) combined with a comparatively low vapour pressure (boiling point  $2270^{\circ}\text{C}$ ) are very convenient experimentally.

Particular attention has been paid to the cathode fall  $V_c$ , as this is probably the most characteristic feature of an arc discharge.

A new method of measuring  $V_c$  has been developed which promises wide application in future arc work.

## CHAPTER II. APPARATUS.

### 2.1. Simple Arc Tube.

To gain experience in the behaviour of arcs, and the experimental techniques involved, a number of experiments were carried out in a very simple arc tube, fig.3. A number of electrode materials were used, cooled and uncooled, (e.g. graphite, tungsten, copper) in various gases (argon, nitrogen, air).

Stabilisation of the arc column was most easily achieved by enclosing the arc in an insulating tube; cooled quartz and uncooled quartz or alumina proved successful and enabled reproducible voltage-length and voltage-current characteristics to be obtained.

The most convenient atmosphere proved to be argon since the arc voltage was low, the arc was fairly stable and deterioration of the electrodes was a minimum. Since argon is monatomic gas, the system is as simple as possible. All measurements are carried out in argon at 760 torr unless otherwise stated.

### 2.2. Demountable Vacuum System.

In the simple arc tube described above, the gas composition was not carefully controlled and it was not possible to clean out the arc vessel by evacuating it. Some experiments had been carried out in argon with tin pool cathodes, these emitted a considerable quantity of 'smoke' and at the time it was not

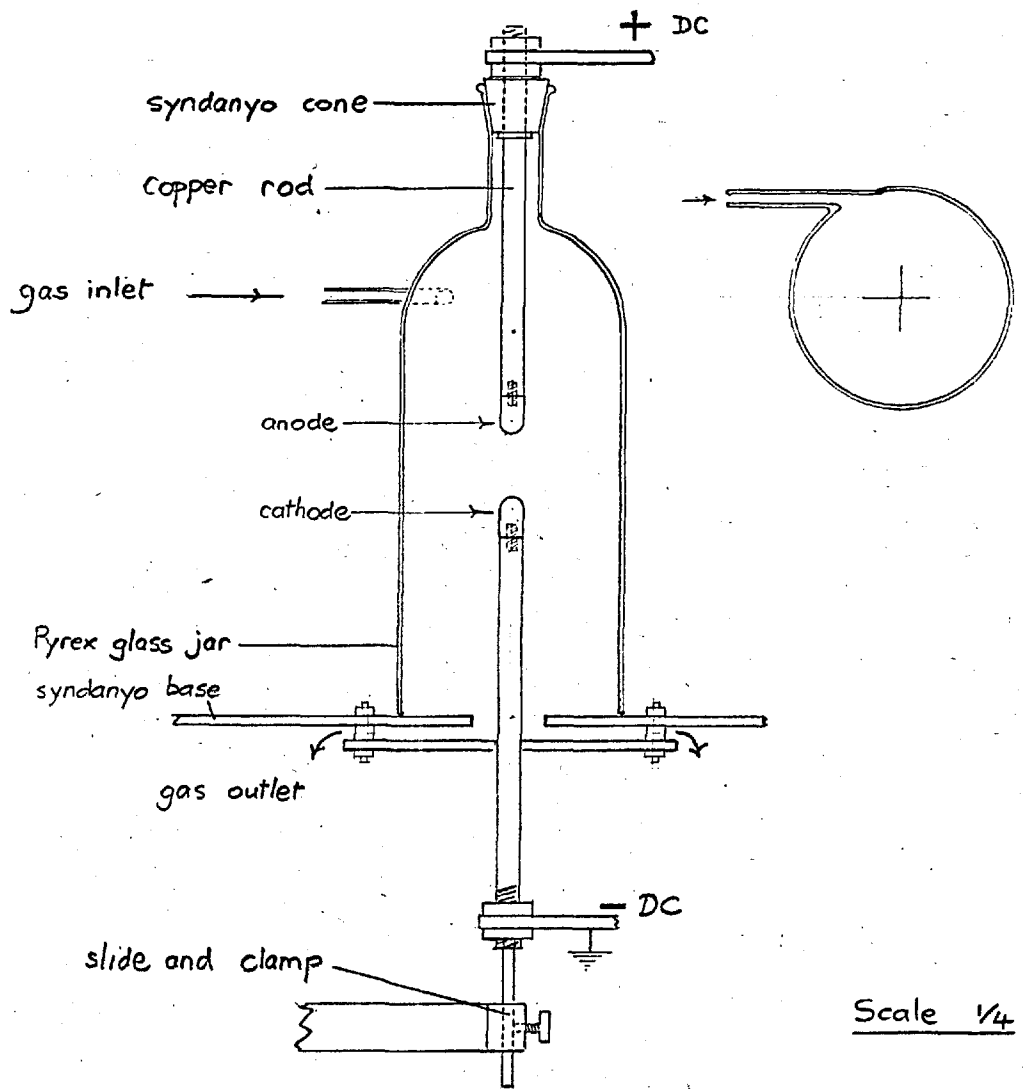


Fig 3. Simple arc tube.



obvious whether this was due to chemical reaction or was simply an inherent property of the tin pool cathode.

Accordingly, some experiments were carried out with very clean glass systems which could be baked under high vacuum, and then filled with dried 99.995% argon to 760 torr. A number of complications were involved in this, such as moveable electrodes to strike the arc. The tin pool cathode still emitted copious smoke under clean conditions indicating that this is a characteristic property of the tin pool arc, and X-ray powder diffraction analysis confirmed that the smoke was pure tin.

An arc tube was then constructed (fig.4) incorporating the following essential features:

- (1) easily demountable,
- (2) could be evacuated to diffusion pump standards,
- (3) unintentional rise in pressure inside the tube due to overheating, not drastic,
- (4) electrodes water-cooled and interchangeable,
- (5) at least one of the electrodes moveable during experiments and for starting the arc,
- (6) able to operate at atmospheric pressure, and remain at that pressure, even when the gas was heated by the arc,
- (7) able to operate at reduced pressure.

Since a system with a continuous gas flow through it is not easily applicable at reduced pressures, a static system was chosen,

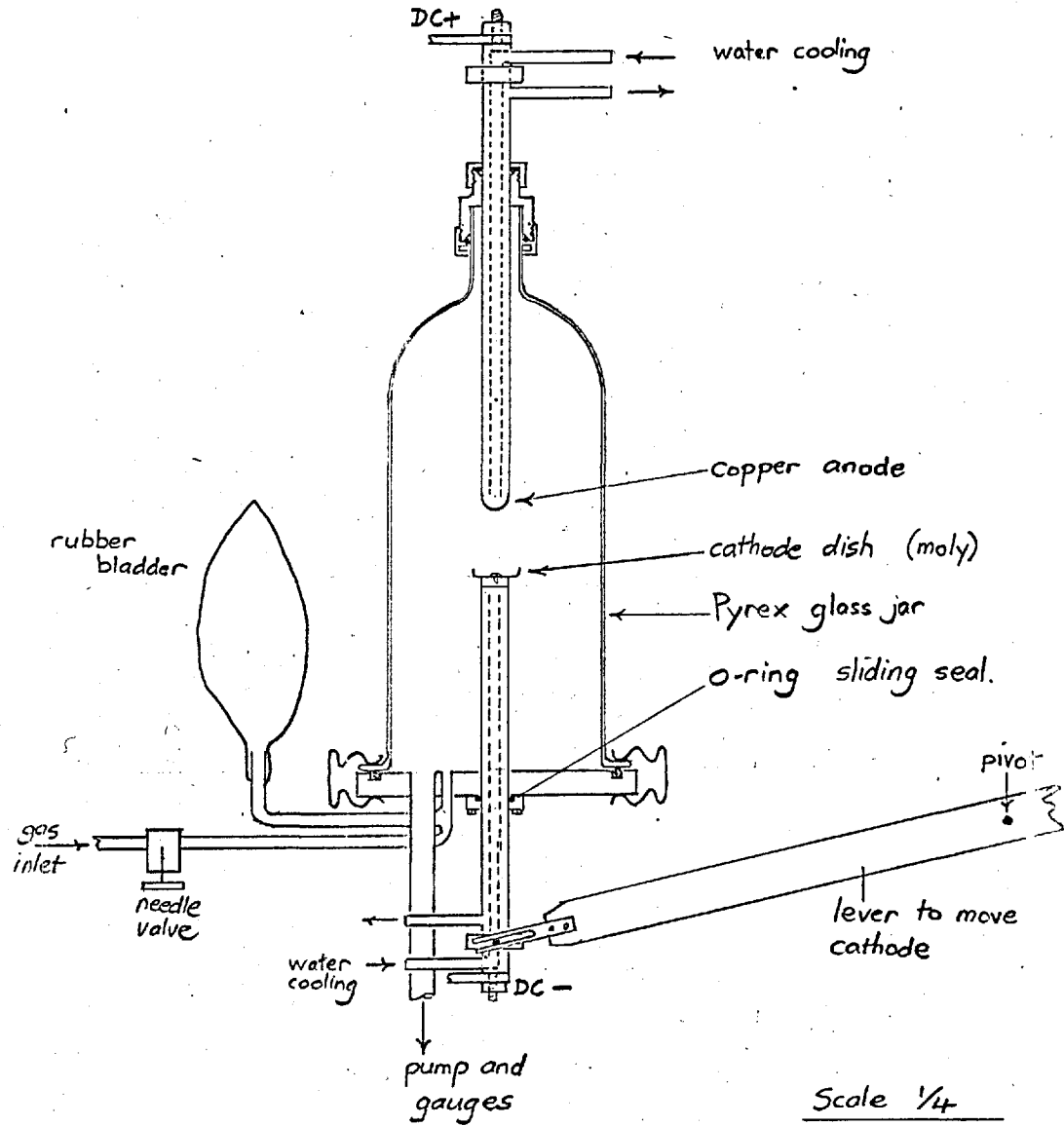


Fig 4. Demountable arc tube.

with expansion of the gas at atmospheric pressure being taken up by a rubber bladder. The vacuum and sliding seals were greased rubber O-rings and the system could be evacuated to  $2 \times 10^{-4}$  torr (the bladder preventing a lower pressure) before being filled with dried gas.

The power supply was a 100 volt, 100 ampere solid state rectifier set controlled by a variac. A heavy current stepped resistor (up to 6 ohms) was placed in series with the arc, and to obtain the most stable arc, as many volts as possible were dropped across the resistor at all times.

### 2.3. Further Modifications.

As the work progressed, limitations of the system became evident; it was often a nuisance to have the lower electrode moveable since attachments such as heaters, thermocouples and probes were often required and it was convenient to attach them to the baseplate, but they usually had to have a fixed relationship to one of the electrodes - usually the cathode. Accordingly, the apparatus was modified so that the upper electrode was moveable during experiments; this was achieved by building a 'Handy Angle' frame around the tube, fig.5, and the whole apparatus was then more rigid and manageable. Also it was now easy to use a displacement transducer (Honeywell LD14) to measure accurately, easily and continuously the electrode gap; and in conjunction with a screw, driven by a constant-speed electric motor, to increase the arc

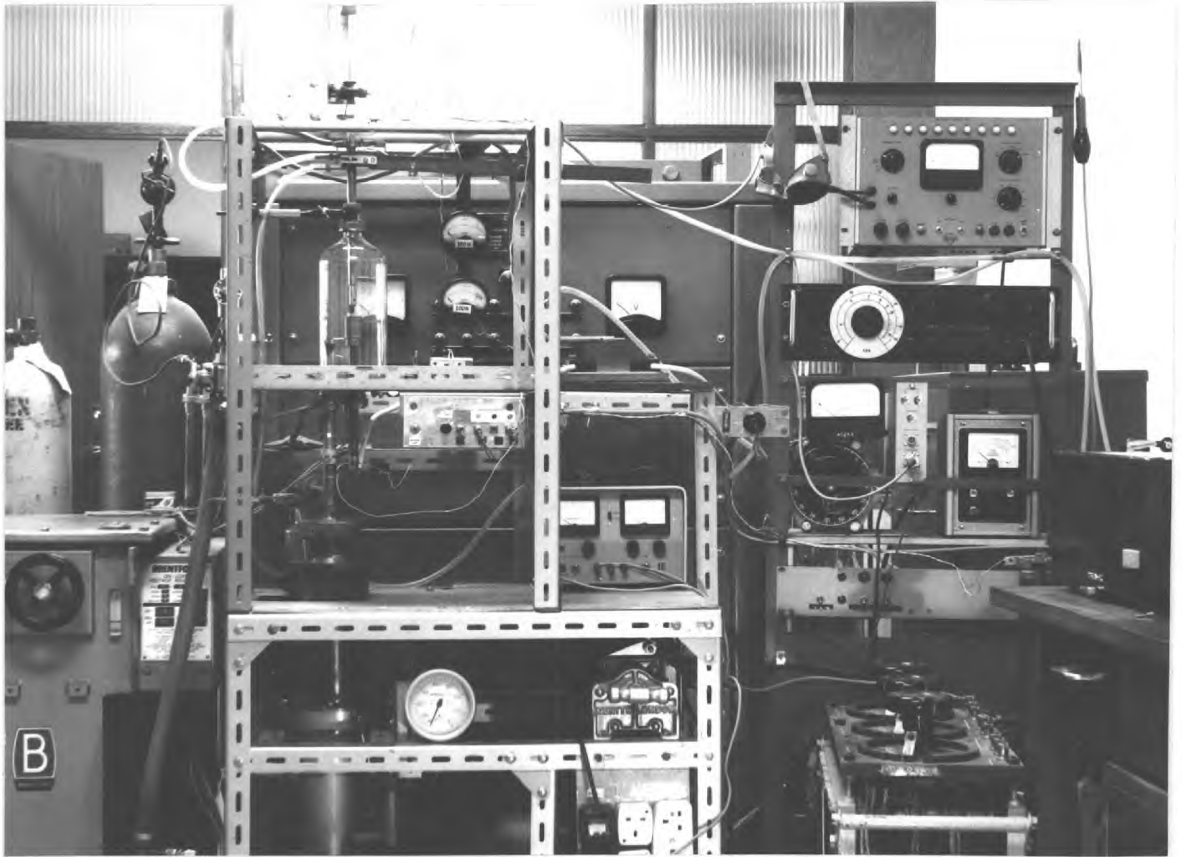


Fig 5. The apparatus.

length at a constant rate, enabling voltage-length characteristics to be plotted using a multi-channel pen recorder.

CHAPTER III. DESIGN OF A TIN DISPENSER CATHODE.

3.1. Tin Pool Cathode and Anchoring Experiments.

A tin pool in a molybdenum dish provided the cathode for the first experiments. The anode was water-cooled copper. With the circuit shown in fig.6 an arc of 10 amperes was drawn by separating the electrodes. The cathode spot was mobile and multiple; tin was ejected from the pool in the form of large droplets (up to 1 mm diameter) and also fine smoke.

It is possible to 'anchor' the cathode spot of a mercury arc by providing a wetted piece of metal (e.g. molybdenum) projecting through the pool surface;<sup>29</sup> the cathode spot then takes the form of a bright line along the wetting edge and mass loss from the cathode is much reduced due to the absence of large drops in the ejected material.<sup>30</sup> Attempts were made to anchor the tin cathode spot; wetting of molybdenum and other metals occurred readily under the influence of the arc, but, although many configurations were attempted, no reliable anchoring was observed in the range 5 to 50 amperes, in argon at atmospheric pressure.

Occasionally, on starting the arc at fairly low currents (i.e. less than 10 amperes) it was observed that a short time elapsed before smoke was emitted from the cathode. On one occasion, this period without smoke was quite prolonged - probably about 30 seconds. This suggested that a 'smokeless' mode of operation may exist, but the condition was not reproducible.

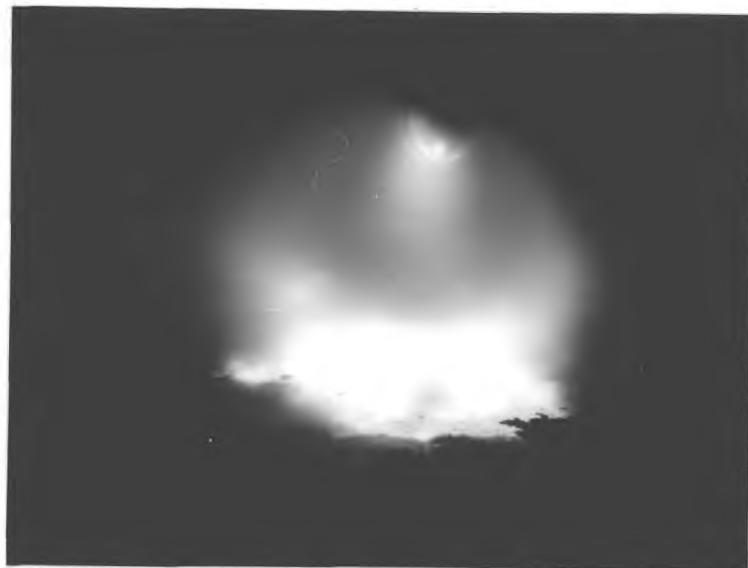
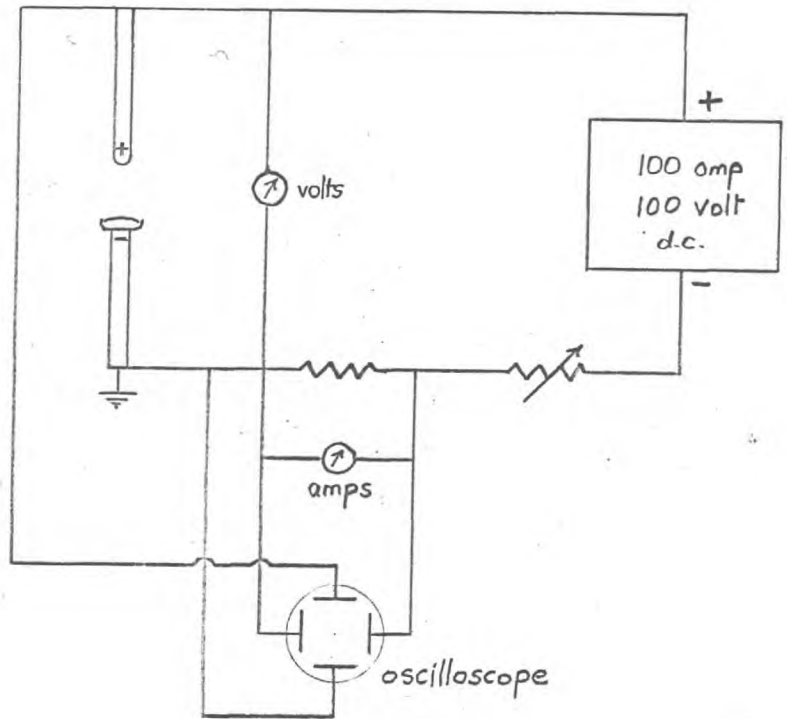


Fig 6. Circuit for current-voltage measurements, and photograph of the tin pool arc.

### 3.2. Wick Cathodes.

Wick cathodes, in which a liquid metal is fed through a high melting point porous metal substrate at the rate at which it is consumed, represent an alternative approach to controlling the cathode spot of a vapour arc. In this case also, ejection of large droplets from the cathode may not take place.

A wick cathode of tin was made from a bundle of molybdenum wires, 0.65 mm diameter and 7mm long. These wires were cleaned electrolytically, tightly clamped in a ring of sheet molybdenum, fig.7, and placed in a tin pool. An arc was drawn from the top of this device and allowed to burn for several minutes at a current of 5 to 10 amperes, after which treatment the wires had become coated with tin.

The results of these experiments were very encouraging; the arc, at first seldom wandered from the dispenser cathode surface, especially at currents above about 20 amperes. There was however an annoying tendency for the surrounding pieces of molybdenum to become coated with tin and act as cathodes. Much tin was evaporated, but mainly as a fine powder which deposited on the inside of the arc chamber.

The arc was maintained at lower currents than usual - 2 amperes as opposed to 10 amperes for a pool - and although the cathode spot was not anchored in the usual sense of the term, its behaviour was less erratic than on a tin pool. The spot appeared to be multiple, and spread over a fairly large area, about  $0.25 \text{ cm}^2$ .



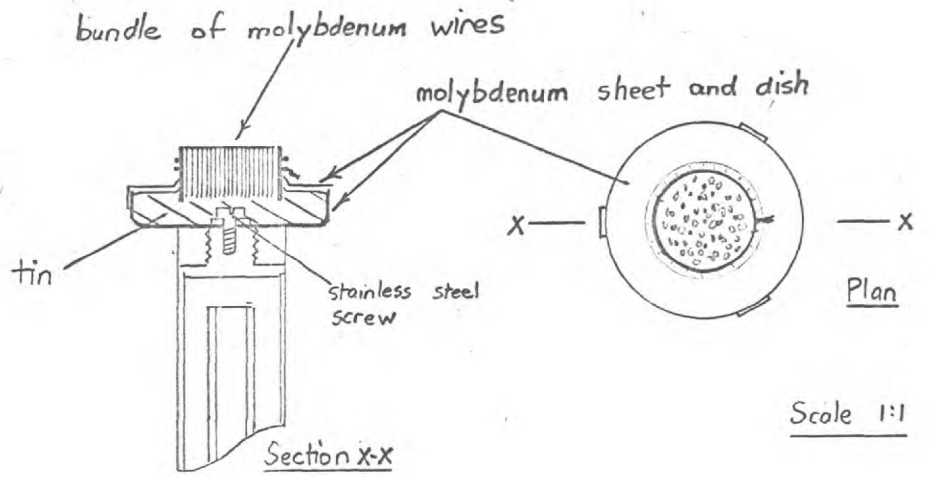


Fig 7. Wires 'wick' cathode.

### 3.3. Porous Discs.

It appeared to be advantageous to try and use a porous disc as the wick, and thus obtain a slower and more controllable supply of tin. Stainless steel discs of various porosity are obtainable commercially (Bound Brook Ltd.) and attempts were made to manufacture porous molybdenum discs in this laboratory by pressing and sintering molybdenum powder. Molybdenum powder was pressed in a 1" diameter steel die at 1 ton/in<sup>2</sup> - the lowest pressure which would give sufficient green strength - and then sintered in vacuo for 30 minutes at 1400°C. These discs, irrespective of initial powder size, were about 50% porous, but their permeability was too low. Two different grades of molybdenum powder were used, the first consisted of particles which would pass through a sieve of 60 B.S. mesh (aperture size 0.0030") but not through one of 200 B.S. mesh (aperture size 0.0099"); the second powder used was coarser being that which did not pass through 60 B.S. mesh (maximum particle size about 0.01"). The permeability of the discs was compared by measuring the rate of rise of pressure in a fixed volume as air leaked through the disc. The disc was sealed onto the vacuum system by a lightly greased O-ring and the enclosed volume evacuated as far as possible with a rotary oil pump. The ultimate pressure obtained, and the rate of rise between two chosen pressures when the pump was shut off by a tap, gave an indication of the permeability. The commercial stainless steel discs were used as standards since their permeability was known. The pore size

required for a 10 ampere arc proved to be of the order of 20 microns.

Before the porous discs were used, they had to be thoroughly wetted and soaked with tin; this was achieved by heating the disc and tin in vacuum with the induction heater to about 800°C, until the tin was seen to soak into the porous metal. The discs could be machined to size and faced-off after soaking.

#### 3.4. Mounting the porous Discs.

The wire wick cathode had suffered from overflowing of tin and the arc tended to wander from the cathode surface onto other parts which had become wetted with surplus tin. In mounting the porous discs the following points were kept in mind:

- (1) the porous disc should be sealed round its edge,
- (2) molten tin under a little pressure should be in contact with the underside of the disc,
- (3) it should be easy to replenish the tin supply.

To satisfy these requirements a U-tube device was made, fig.8(a), consisting of a copper block, drilled out as shown, with the pre-soaked porous disc clamped onto the open end of the lower arm and sealed round the edges with alumina+potassium silicate cement. Tin was introduced before the disc was clamped into place (and subsequently into the open arm) and melted by a heating coil in the block. A molybdenum-constantan thermocouple measured the block temperature. The longer arm was protected from the arc

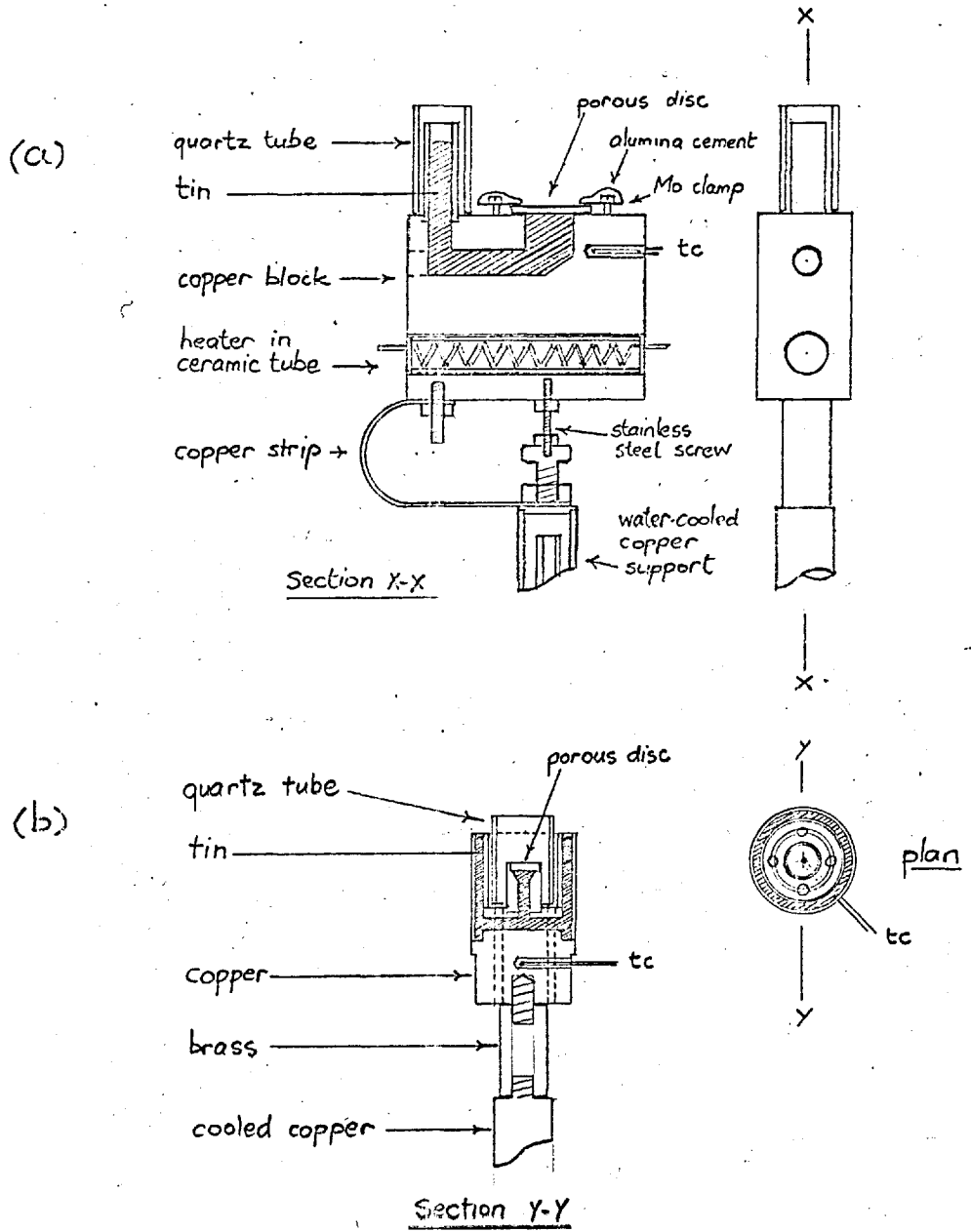


Fig 8. U-tube dispenser cathodes.

by a quartz tube, and other exposed parts were coated with a thin layer of alumina cement.

This cathode was later modified to make it cylindrically symmetric and so encourage uniform gas flow around the arc column and thus increasing its stability. Fig. 8(b) shows this cathode, constructed from copper; the cathode surface was made smaller than previously to try and limit the wandering of the cathode spot. The tube without the cathode disc in place was filled with tin and heated to about 250°C in vacuum to clean up the tin and drive off any air bubbles. A previously tin-soaked porous disc was turned to be a push fit in the recess bored for it, and finally more tin was added between the two outer tubes so that the level there was above the cathode surface. A quartz tube prevented the arc from striking to the outer tubes. The cathode was mounted, via a brass rod, on the water-cooled support, the length of the brass being such that the heat input from the arc, assuming a current of 10 amperes and a cathode fall of 10 volts, would be sufficient to maintain the cathode at 240°C. At a later date a heater was added around the cathode to prevent deterioration of its surface, due to operation before the tin was molten.

In the final design of dispenser cathode a stainless steel tube, 3/8" external diameter, was obtained and a recess bored in one end to take an unsoaked porous stainless steel disc. By arranging a moveable pointed tungsten electrode (as anode) so that it could travel around the join, it was possible to argon arc weld

the disc into the tube. The cathode was then tested under water with compressed air, and finally soaked in tin by suspending in vacuum, with tin inside, and heating until the tin dripped through the porous end.

### 3.5. Behaviour of the Tin Dispenser Cathode.

Without a doubt, the cathode spot is less erratic on such a cathode than it is on a tin pool, and also an arc can be sustained at a lower current. This must be weighed against the difficulty in obtaining the optimum supply rate of tin. It seems likely that the cathode would operate satisfactorily only in a narrow current range ( $\pm 5$  amperes) for any particular porosity.

An estimate of the tin evaporation rate from a porous disc dispenser cathode was made by weighing the cathode before and after a run of 30 minutes at a current of 10 amperes. The result was  $10^{-4}$  grams per coulomb. This is of the same order as obtained from an anchored mercury spot, but rather more than obtained from copper<sup>13</sup>.

Though the stainless steel discs are adequate for experimental purposes, their life is too short for practical application; attempts would have to be made to obtain porous refractory metals of high permeability.

In spite of its possible practical limitations, this type of cathode is a very convenient form for studying liquid cathode vapour arcs; it was in this light that this research program was

developed. The cathode spot is sufficiently still to make possible a number of measurements which are rather difficult with a free spot on a pool cathode.

### 3.6. Electrical Characteristics.

Voltage-length plots for various types of tin cathode are shown in fig.9 with the circuit in fig.6. It seems immaterial whether the tin is in the form of a pool or a dispenser - the arc voltage is the same, within the scatter of the results. A potential of about 20 volts is indicated for the total electrode fall but since this includes the contribution of the contracted parts of the column close to the electrodes this result has limited interest.

A typical voltage-current plot is given in fig.10. The shape is typical of arc discharges, in general<sup>31</sup>.

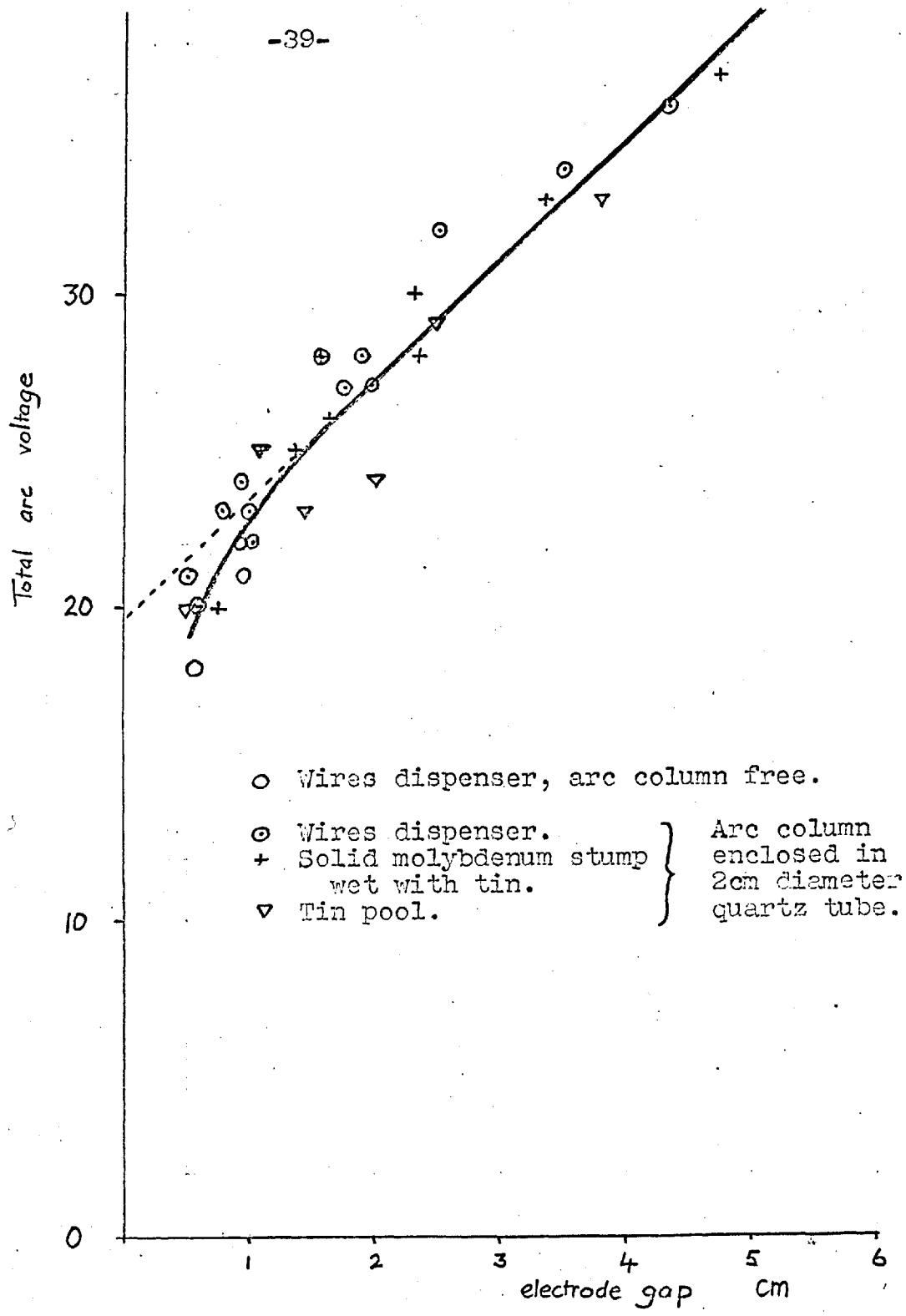


Fig 9. Voltage-length characteristics for tin arcs. Current 10-30 amperes. Argon, 760 torr. Cooled copper anode.



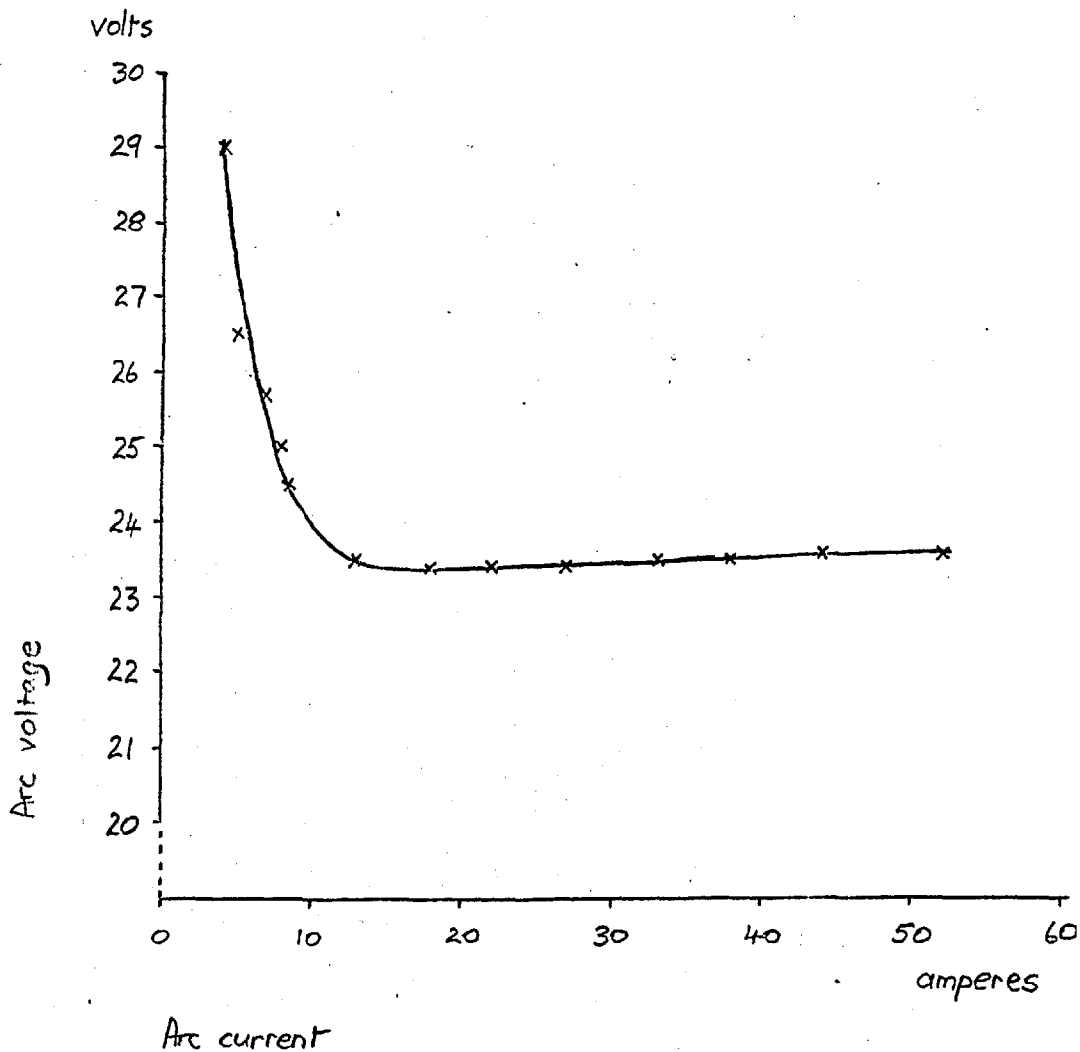


Fig 10. Current-voltage plot for concentric U-tube type tin dispenser cathode.  
Argon, 760 torr.  
Cooled copper anode.  
Arc length: 1cm.

CHAPTER IV. PROBE MEASUREMENTS.

4.1. Purpose.

A voltage-length plot for lengths greater than 3-5 mm, extrapolated to zero length, gives a voltage equal to the sum of the anode and cathode falls together with a voltage contribution from the contracted parts of the arc column close to the electrodes, where the voltage gradient is greater than that in the positive column, but which do not actively contribute to the mechanisms at the electrodes,  $V_c + V_a + V_x + V_y$  in fig. 11, where  $V_x$  and  $V_y$  are the differences between the extrapolated and actual values of  $V_c$  and  $V_a$  respectively.

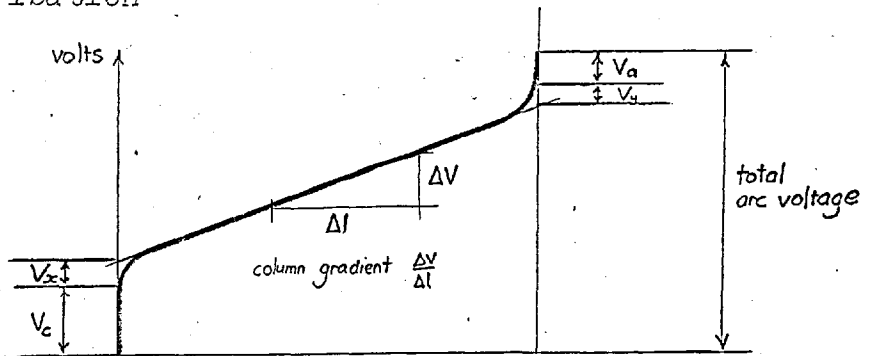
If the arc gap is closed until the electrodes contact, while the arc voltage is recorded (e.g. on an oscilloscope), an abrupt drop of voltage is experienced as the electrodes meet<sup>14</sup>; the value of which gives an estimate of  $V_c + V_a$ .

Neither of these methods permit separate measurements of  $V_c$  and  $V_a$ . If the column voltage gradient is known (and this is easily measured by altering the arc length) then a determination of the potential at a known point in the column would enable  $V_c + V_x$  to be separated from  $V_a + V_y$ . This at least would be a start in separating  $V_c$  and  $V_a$ .

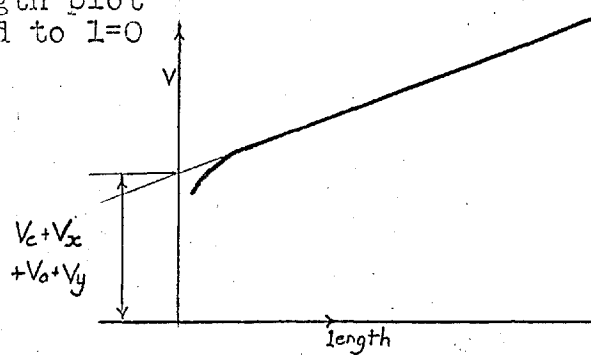
In low pressure gas discharges, probes find widespread application enabling the space potential and electron temperature in a plasma to be ascertained. It was hoped that a probe could



Potential distribution



Voltage-length plot extrapolated to  $l=0$



Voltage as the electrodes are brought together

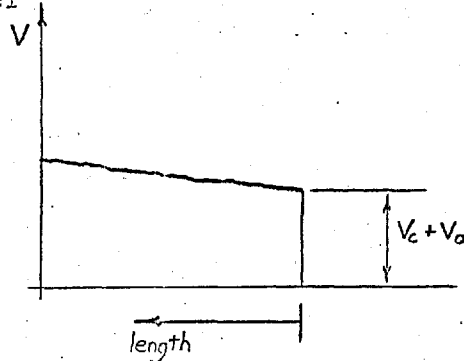


Fig 11. Definition and measurement of the electrode falls.

be used to measure the potential at a known point in the arc column.

#### 4.2. General Theory of Probe Measurements.

It is not proposed here to go into great detail since the information is available elsewhere<sup>32</sup> and much of it is inapplicable at high pressures. The method was developed by Langmuir<sup>33</sup>, and bears his name.

If a probe (e.g. a fine wire) is inserted into a plasma and connected as in fig. 12, and the current in the probe circuit is measured as a function of applied probe voltage, then a characteristic curve as indicated may be obtained. This may be explained qualitatively as follows, the numbers referring to fig.12.

When the probe is negative with respect to the plasma, electrons will be repelled and ions attracted, resulting in a positive space charge round the probe visible as a dark sheath at low pressures, and a saturated ion current is collected (1). As the probe is made less negative, electrons will be able to reach it, at first only the fastest ones, and the probe current starts to decrease (2). As the probe is made less negative, the current to it will pass through zero (3), when equal numbers of ions and electrons are collected, and then increase again (4) in the reverse direction as the number of electrons exceeds the numbers of ions collected. When the probe passes through the

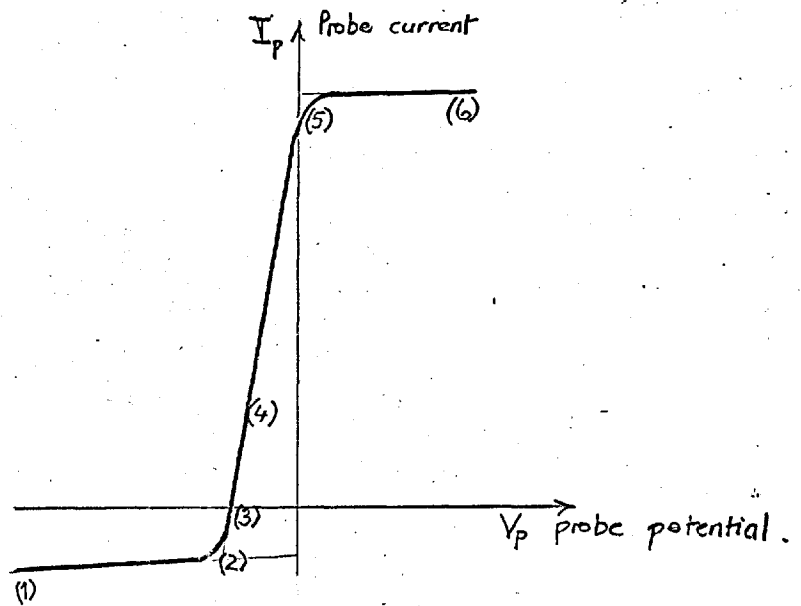
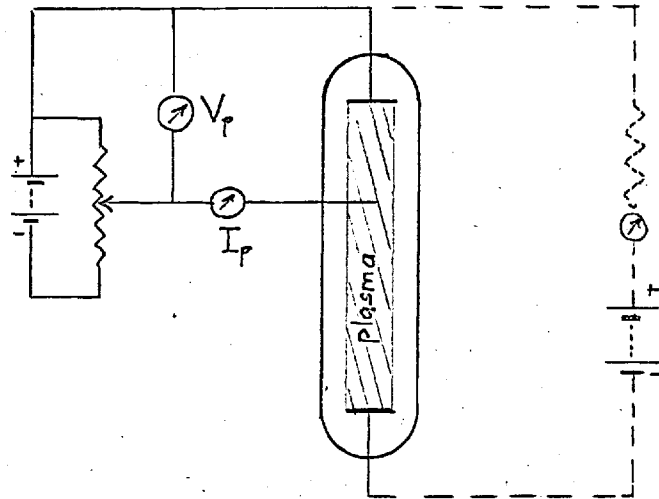


Fig 12. Method for making Langmuir probe measurements, and a typical probe current-voltage characteristic.

plasma potential (5), the positive ion sheath disappears, and as the potential is made more positive (6), it is replaced by a sheath of electrons and a saturated electron current is collected. The potential at the 'knee' in the curve gives the space potential.

The slope of the curve between (4) and (5) is a measure of the number of electrons with sufficient energy to overcome the repulsive probe potential; it gives the electron temperature if the velocity distribution of the electrons is Maxwellian.

In the interpretation of probe measurements certain assumptions are made:

- (1) no collisions in the space charge sheath,
- (2) all ions and electrons reaching the probe surface are absorbed,
- (3) the discharge is not disturbed significantly by the presence of the probe.

#### 4.3. Previous Probe Measurements on Arcs at High Pressures.

In attempting to use a probe in the column of an atmospheric pressure arc, a number of difficulties arise - not the least being that a stationary probe will melt, since the gas temperature in the arc is above the melting point of all known metals. However, probes have been used in the past with varying amounts of success. The problem of melting is overcome by moving the probe rapidly through the arc, but this introduces further problems as the probe is no longer in thermal equilibrium with the plasma.

Nottingham<sup>34</sup> in 1928-29 measured the total charge picked up by a probe as it passed through an arc; he applied various potentials to the probe and measured the charge on a ballistic galvanometer. In 1932, Bramhall<sup>35</sup> carried out Langmuir probe measurements, using a platinum probe swung through an arc in air with copper electrodes. He concluded that the column gradient was non-uniform, but this is hardly surprising since his arc length was only 4 mm. He estimated the cathode fall  $V_c$  to be 11-13 volts, but the arc voltage increased by 1-6 volts as the probe passed through the arc column. A similar voltage increase was also observed by Mason<sup>36</sup> about the same time.

A probe consisting of a continuous wire wound from one spool to another, was used by Mason<sup>37</sup> in 1937. This wire could be positioned in the same way as a stationary probe, but its temperature was below the gas temperature, resulting in a dark (i.e. cool) space around the probe, the size of which was found to be independent of probe potential within wide limits and so must be of thermal origin. He concluded that the voltage increase was due to energy from the arc being transferred to the probe by thermal conduction and by recombination of dissociated molecules at the probe surface. He considered that the presence of the dark space made interpretation of results unreliable.

Recently, Cozens and von Engel<sup>38</sup> have shown how high pressure probe measurements may be interpreted.

#### 4.4. Flying Probe Measurements.

With the aim of separating the anode fall  $V_a$  from the cathode fall  $V_c$  by finding the space potential at a known point in the arc column, a 'flying probe' was constructed, fig.13. By means of a spring, the probe could be made to travel rapidly across the arc column. The movement was controlled by a mechanism which could be set and released from outside the arc chamber. The probe potential and current were recorded on an oscilloscope, the timebase of which was triggered at the moment of releasing the probe, and the delayed timebase adjusted to scan when the probe passed through the arc column (this facility on the Tektronix 561A oscilloscope enables any small part of the trace to be expanded to the whole width of the screen). The probe was 0.65 mm diameter tungsten wire and its speed ( $\sim 300$  cm/sec. at the tip) was rather arbitrarily determined by the springs available at the time.

At first the probe was used floating to get some idea of the arc disturbance. The increase in arc voltage as the probe passed through the arc was recorded along with the probe potential. For an arc 0.5 cm long, carrying 10-30 amperes, and the probe midway between the cathode and anode, the probe reached a floating potential of 10 volts and the arc voltage increased by 3-5 volts (in 20 volts) when the probe crossed the arc axis.

From these results, it was apparent that with this probe speed, characteristics would have to be plotted in less than a millisecond. Slowing down the probe would give a longer time to



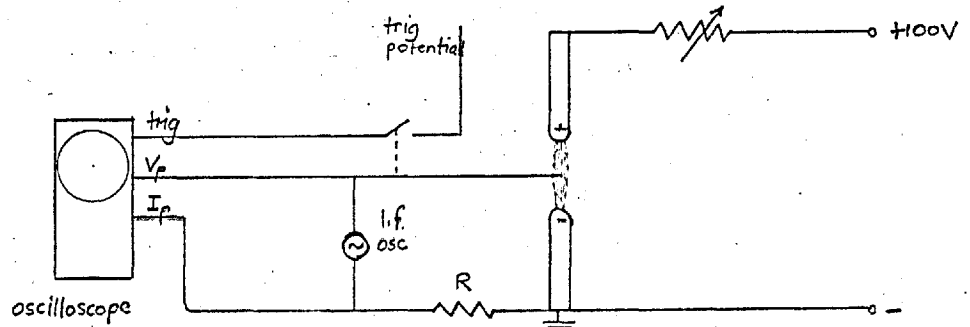
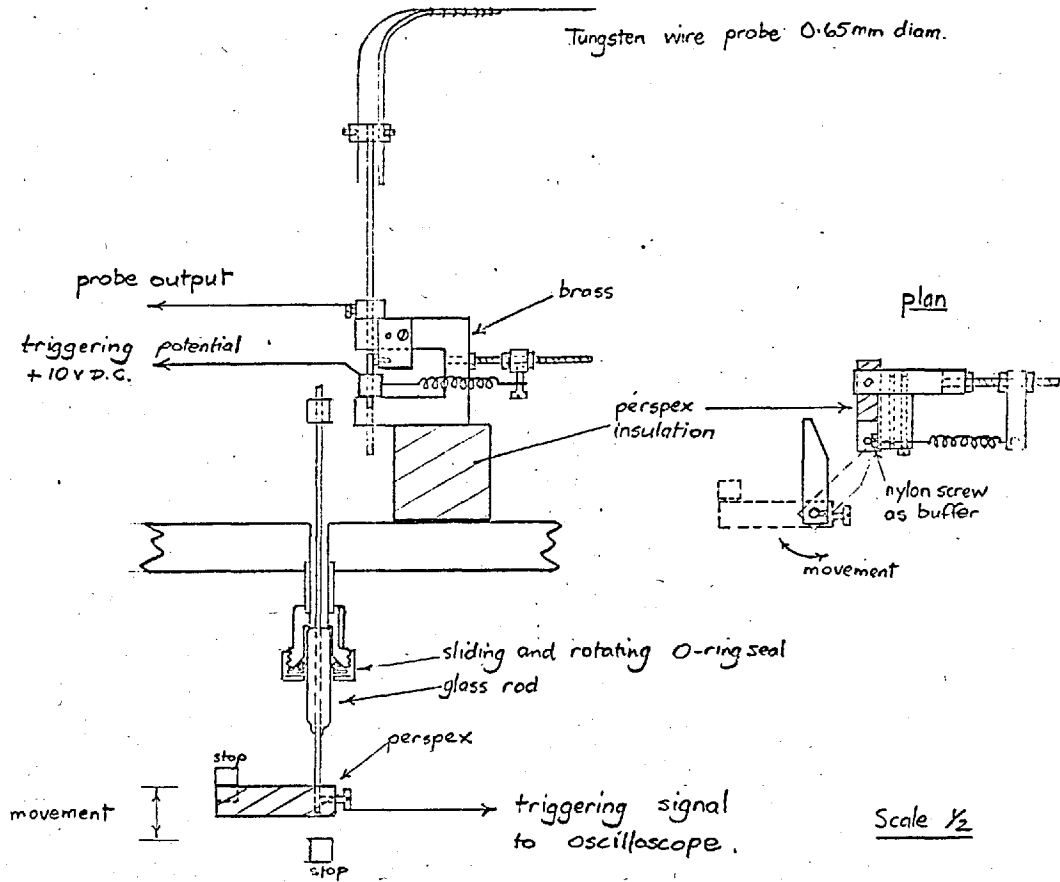


Fig 13. Spring-loaded flying probe.

take measurements, but there is then more risk of the probe becoming hot enough to melt or emit electrons. The circuit used to plot probe current-voltage characteristics is given in fig.13. A low frequency oscillator was used to vary the probe voltage and the resulting probe current was measured and displayed on the oscilloscope, as the voltage across a series resistor. The trace was photographed. Current-voltage characteristics were obtained, with the probe potential varied at 250-1,000 cycles/sec, but it was difficult to ensure that the characteristic was being plotted at the appropriate millisecond when the probe was in the centre of the arc column. It was hoped to rectify this by means of a rotating probe.

#### 4.5. Rotating Probe.

If a probe is rotated so that one point is plotted each time it passes through the arc column, there can be no doubt that the probe is in the centre of the arc column during a measurement, since the peak value of the probe current pulse can be measured. Also with the rotating probe it was possible to experiment with different probe speeds and thus choose the slowest convenient rate. A probe, fig.14, was made which rotated at 275 revs/minute (giving a speed of 40 cm/sec. at the tip), at which speed the probe remained cool under most conditions.

It proved rather difficult to record the peak of the pulse as the probe passed through the arc, since its width was only about

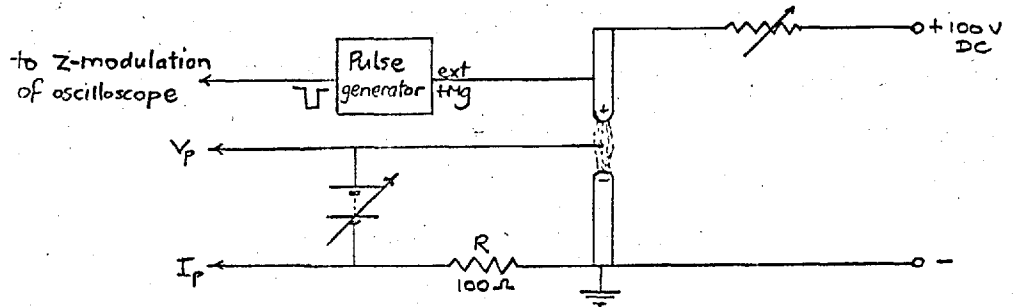
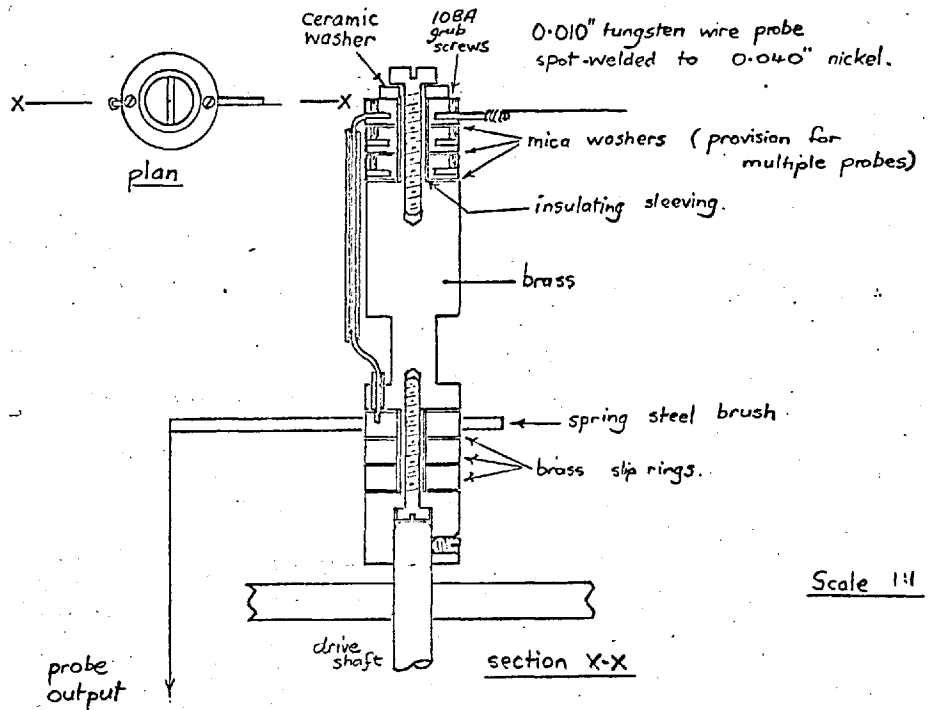


Fig 14. Rotating probe.

one hundredth of a rotation and the brightness control of the oscilloscope had to be turned up so much that the base line (when the probe was outside the arc) was excessively bright. Success was achieved by using the increase in total arc voltage due to the probe passing through the arc to trigger a pulse generator, the output from which operated the z-modulation (brightness) of the oscilloscope, and a characteristic obtained thus is shown in fig. 15. The voltage applied to the probe was altered manually, while the oscilloscope camera shutter was held open. The oscilloscope was fitted with a differential amplifier on both axes, so that current-voltage characteristics were obtained directly. The ion current and electron current were measured on separate runs with different current sensitivities. Current and voltage values were taken from a smooth curve drawn through the experimental points and used to make a plot of the logarithm of the electron current versus probe potential, fig.16. Conclusions from this will be discussed later.

#### 4.6. Probe Theory at High Pressures.

The fundamental difference between the behaviour of current carrying probes at high and low pressures has been discussed by Cozens and von Engel.<sup>38</sup>

At low pressures, a space charge 'sheath' exists around the probe which electrons and ions cross without collision, the probe acting as a velocity selector, collecting those electrons having

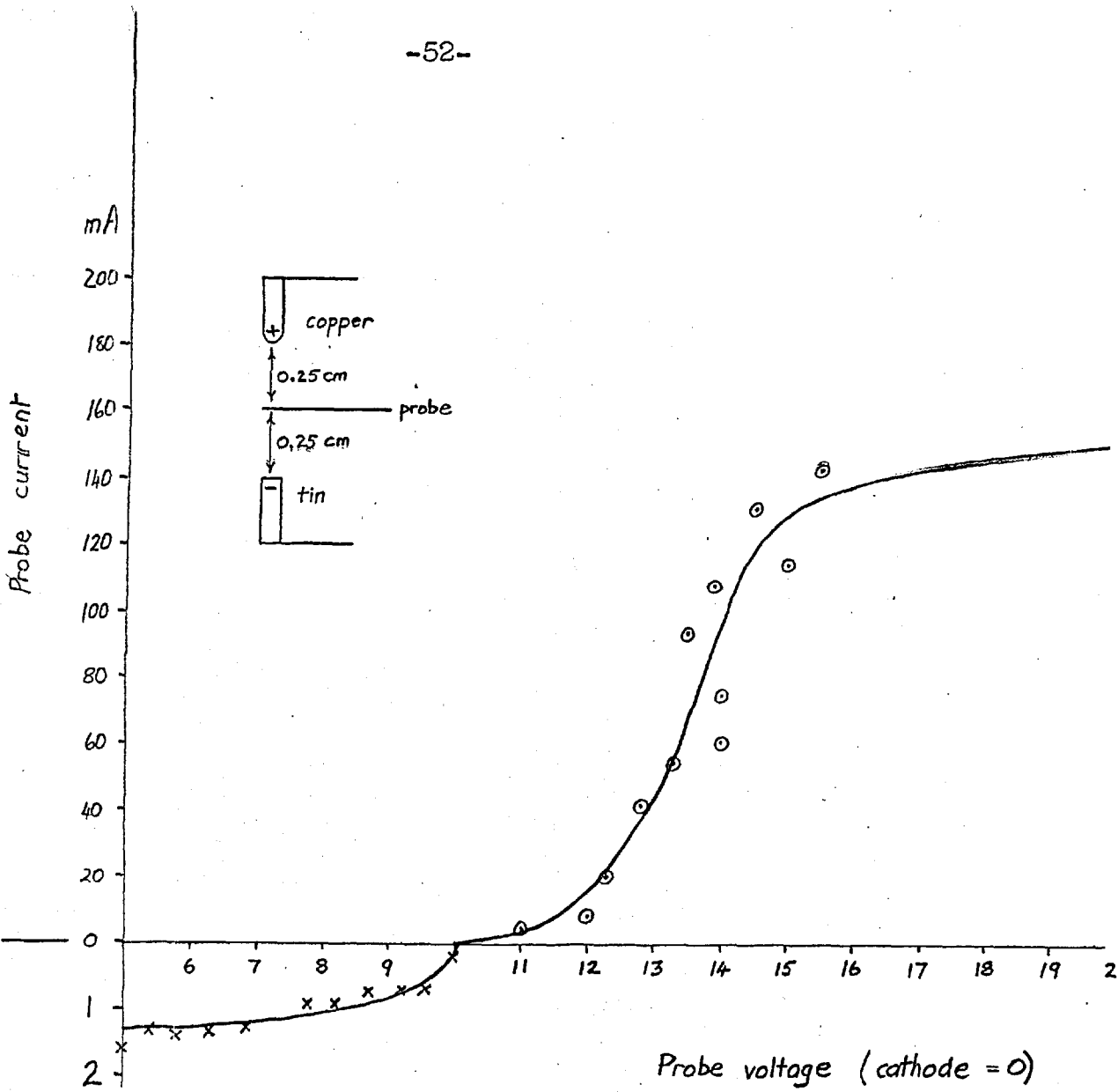


Fig 15. Probe current-voltage characteristic. Tin dispenser cathode, cooled copper anode. Argon at 760 torr. Current: 10 amperes.

Probe: 0.050 cm diameter tungsten. Surface area in arc: about 0.05 cm<sup>2</sup>. Rotating at 275 rpm.

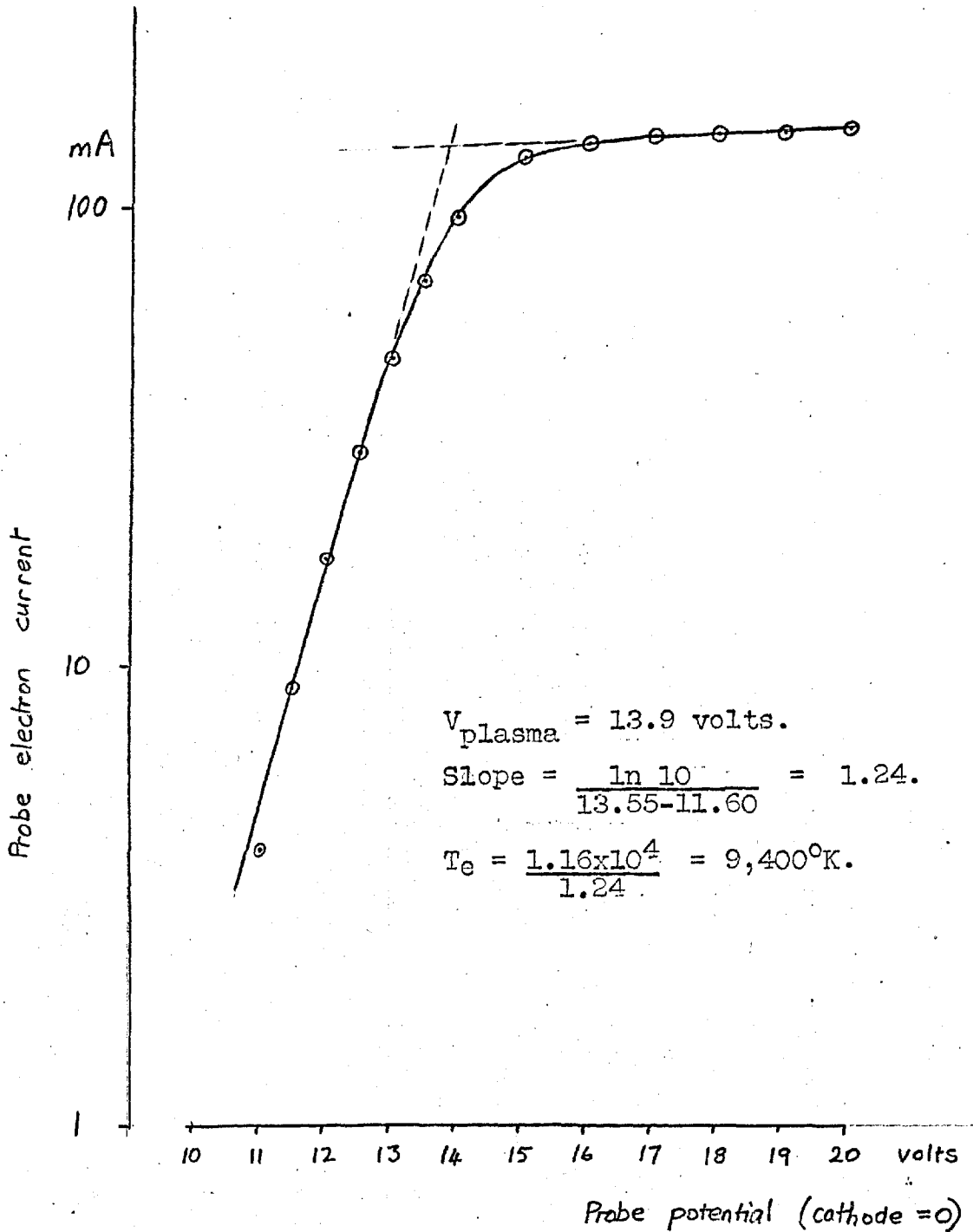


Fig 16. Semi-log plot obtained from the smooth curve of fig 15.

sufficient perpendicular energy to overcome a repulsive probe potential. In this case, the number of electrons reaching the probe at a given probe potential  $V_p$ , negative with respect to the plasma (in the region 4 of fig.12), is given by the Boltzmann relation:

$$n_p = n_o \exp \frac{-eV_p}{kT_e}$$

where  $n_p$  is the electron concentration at the probe surface,  
 $n_o$  " " " " in the body of the plasma  
 = " " " " at sheath/plasma boundary,  
 $T_e$  is the electron temperature.

Hence the electron current density to the probe is:

$$j_- = j_o \exp \frac{-eV_p}{kT_e}$$

where  $j_o$  is the random electron current density at the sheath boundary and is equal to  $\frac{1}{4}n_o\bar{v}_-$ , where  $\bar{v}_-$  is the mean electron velocity given by  $(8kT/\pi m)^{\frac{1}{2}}$ .

$$\therefore \ln j_- = \ln j_o - \frac{eV_p}{kT_e} \quad \text{and since } \ln j_o \text{ is constant,}$$

$$\frac{d(\ln j_-)}{dV_p} = - \frac{e}{kT_e}$$

so that the electron temperature is obtained from the slope of a plot of the logarithm of the probe electron current density versus probe potential. The ion current density meanwhile is constant.

At high pressure, when the electron mean free path is much less than the expected sheath size, or 'region of influence' of the probe potential, then account must be taken of collisions. The following account follows the treatment by Cozens and von Engel<sup>38</sup>. The motion of the electrons and ions can then be described by diffusion and mobility considerations. The electron and ion current densities are given by:

$$j_- = -D_- e \frac{dn_-}{dx} + \mu_- n_- e \frac{dV}{dx}$$

and  $j_+ = -D_+ e \frac{dn_+}{dx} - \mu_+ n_+ e \frac{dV}{dx}$  respectively,

where  $D_-$  and  $D_+$  are diffusion coefficients,

$\mu_-$  and  $\mu_+$  are mobilities,

$n_-$  and  $n_+$  are concentrations,

and  $x$  is measured perpendicularly into the probe (at  $x = x_p$ ) from the undisturbed plasma.

If the probe is floating (i.e. drawing no net current) then

$j_- = j_+$ , and the flow of charged particles to the probe is described by an ambipolar diffusion coefficient

$$D_a = \frac{\mu_+ D_- + \mu_- D_+}{\mu_+ + \mu_-}$$

resulting in an electron density distribution  $n_- = n_0 \cos ax$  where  $a^2 = z/D_a$  and  $z$  is the number of single ionising collisions per second.



In a steady state:

$$-D_- \frac{dn_-}{dx} + \mu_- N_- \frac{dV}{dx} = z \int_0^x n_- dx$$

and with  $n = n_0$ ,  $V = 0$  at  $x = 0$ ;

$$n = n_p, V = V_w \text{ at } x = x_p$$

$$V_w = \frac{D_- - D_a}{\mu_-} \ln \frac{n_p}{n_0} \quad \text{-----}(\#)$$

If an external voltage is now applied to the probe so that a net probe current density  $j_p$  results, then  $j_- = j_+ + j_p$ .  $j_+$  can be assumed constant and equal to the random ion current density, with the ion density  $n_+$  in front of the probe unchanged. Since more electrons are being collected than when the probe was floating, the electron density at the probe surface will change from  $n_-$  to  $n'_-$  and the previous boundary condition of

$$\frac{1}{4}(n_- \bar{v}_-)_{\text{probe}} = \frac{1}{4}(n_+ \bar{v}_+)_{\text{probe}}$$

becomes

$$\frac{1}{4}(n'_- \bar{v}_-)_{\text{probe}} = \frac{1}{4}(n_+ \bar{v}_+)_{\text{probe}} + j_p/e = (j_+ + j_p)/e,$$

so that  $\#$  becomes

$$V'_w = \frac{D_- - D_a}{\mu_-} \ln \frac{n'_p}{n_0}$$

and the probe potential, relative to the floating potential is:

$$\begin{aligned}
 V_P &= V'_w - V_w = \frac{D_- - D_a}{\mu_-} \ln \frac{n'_p}{n_p} = \frac{kT_e}{e} \ln \frac{j_+ + j_p}{j_+} \\
 &= \frac{kT_e}{e} \ln \frac{j_-}{j_+}
 \end{aligned}$$

$$\therefore \frac{d(\ln j_-)}{dV_P} = \frac{e}{kT_e}$$

which, it turns out is the same form as the low pressure result.

The similarity arises from assuming

$$\frac{D_- - D_a}{\mu_-} \approx \frac{D_-}{\mu_-} = \frac{kT_e}{e}$$

#### 4.7. Discussion of Probe Results.

##### (1) The Space Potential

A probe at the same potential as the plasma may be expected to collect the random current densities of both electrons and positive ions. If the probe potential is made more positive, the positive ions will be repelled but no more electrons can be collected than the random electron current density  $\frac{1}{4}n_-v_-$ . So, in a similar manner to the probe at low pressure, the probe current-voltage curve should have a 'knee' at the space potential. Fig. 16, shows that this occurred at 13.9 volts, say 14 volts, within the limits of accuracy.

The sum of the cathode fall  $V_c$  and the anode fall  $V_a$  was found to be 15 volts, by bringing the electrodes together. The total arc voltage as the probe passed through the arc was 22 volts

(including the voltage increase due to the probe). Therefore, 22 minus 15 = 7 volts is what remains after subtracting  $V_c + V_a$ . Assume that this 7 volts is evenly shared either side of the probe since the probe is equidistant from cathode and anode, then with the potential at the probe position being 14 volts:

$$V_c = 14 - 3.5 = 11.5 \text{ volts}$$

and  $V_a = 15 - 11.5 = 3.5 \text{ volts.}$

Notice that it has been assumed that  $V_x = V_y$ , i.e. the voltage contributions of the contracted parts of the column close to the cathode and anode are equal. There is no experimental justification for this, but it would seem a reasonable first approximation, lacking further evidence.

(2) The Electron Temperature.

The probe theory given above indicates that the electron temperature  $T_e$  should be obtainable from the plot of logarithm  $j_-$  versus  $V_{\text{probe}}$ . This is shown in fig.16, giving  $T_e = 9,400^\circ\text{K}$ . This appears a factor of two large compared with other published data<sup>14</sup>. This suggests thermal equilibrium may not be attained in argon.

#### 4.8. Conclusions.

The space potential in the positive column of an arc discharge may be measured by means of a moving probe, but the disturbance of the arc by the probe, manifesting itself as an increase in arc voltage, must introduce a degree of uncertainty in interpreting the results. However, this disturbance can be usefully employed to trigger a measuring device when the probe is in the centre of the arc column.

Referring to fig. 11, it is fairly easy to separate  $V_c + V_x$  and  $V_a + V_y$  by using a probe, but without a method of measuring  $V_x$  and  $V_y$  separately this does not give sufficient information to determine  $V_c$  and  $V_a$  separately.

Since a far better method of measuring  $V_c$  and  $V_a$  was discovered at about this stage in the investigations (described in the next chapter), there seemed nothing to be gained by proceeding further with probe measurements.

CHAPTER V.      SEPARATE MEASUREMENTS OF THE ANODE FALL AND  
CATHODE FALL.

5.1. Introduction.

In an arc discharge the cathode and anode falls of potential occupy very thin sheaths at the electrode surfaces. Potential measurements are frustrated by the small size of these regions of high current density and strong electric field. In addition, the cathode spot of the vapour arc moves rapidly at random over the electrode surface, although in certain circumstances it may be "anchored".

The sum of the cathode and anode falls has been estimated by moving the anode and cathode rapidly towards one another while recording the total arc voltage on an oscillograph<sup>14</sup>; as the electrode gap decreases, the column becomes shorter and the total arc voltage slowly decreases until, just before contact, the voltage across the electrodes drops rapidly to zero from a value believed to represent the sum of the anode and cathode falls. Alternatively, a voltage-length characteristic extrapolated to zero length may give some indication of the total potential drop at the electrodes, but the arc voltage is not proportional to the arc length except at gaps greater than about 3mm<sup>12</sup> and extrapolation of this line to zero length must give a voltage that includes a contribution due to the contracted regions of the column close to the electrodes where the electric field is higher than in the positive column but still much lower than in the electrode fall spaces. Neither of these methods enables the anode fall and

cathode fall to be determined separately, though a certain amount may be deduced by using a number of combinations of anode and cathode material.

A solution to the problem of measuring separately the anode fall and cathode fall of potential is described below. If the voltage across the arc electrodes is recorded on a high speed oscilloscope as the electrodes are brought rapidly together, and the time scale around the moment of impact can be suitably expanded, then in many cases it is observed that the abrupt voltage drop as the electrodes meet is discontinuous. It is suggested that this discontinuity, or step, in the arc voltage versus arc gap trace permits separation of the anode and cathode falls - something which has not been directly achieved by any other method. Lack of suitable instrumentation explains why early workers in the field did not notice this.

## 5.2. Principle of the Method.

What happens as the electrodes of an arc are brought together?

At the cathode, a very high current density of electrons is emitted, these are accelerated in the cathode fall until they have sufficient energy to ionise or excite the atoms with which they collide. Since the cathode is negative, it repels electrons and attracts positive ions, the result is a positive ion space charge in front of it giving a region of high electric field, the cathode fall.

At the anode, which is electron attracting and ion repelling, there is an excess of electrons, producing a net negative space charge and thus a region of high field, the anode fall.

In a steady state long arc, the two electrode regions are joined by an arc column comprised of neutral atoms and equal densities of positive ions and electrons drifting towards the cathode and anode respectively, under the influence of the applied field. If the electrodes are brought closer together, the total arc voltage will decrease, but nothing can be expected to change in the electrode regions until they start to 'overlap'. At this stage, electrons from the cathode, having sufficient energy to ionise or excite neutral atoms, will be arriving in front of the anode so that positive ions will be produced there and neutralise the negative space charge, i.e. the anode fall disappears. This can be expected to occur owing to the very high current density. The potential difference across the arc electrodes will now simply be the cathode fall alone.

If the number of ions produced in front of the anode is more than sufficient to neutralise the negative space charge then a negative anode fall may arise.

### 5.3. Experimental Details.

The aim is to record the total arc voltage as a function of the anode-cathode spacing for a decreasing arc gap, concentrating on the moment of impact when the arc extinguishes and the anode-

cathode voltage drops to zero. The delayed sweep facility of the Tektronix 561A oscilloscope fitted with a 3B3 timebase plug-in unit permits expansion (along the time scale) of any small part of the trace to the full width of the screen. Thus, providing the moment when the anode and cathode contact can be predicted, it should be possible to record the voltage versus time at that instant on a 'stretched' time scale. The alternative possibility of triggering the oscilloscope timebase directly from the signal was tried first, but owing to the voltage fluctuations and the small gradient of the voltage versus time curve this proved rather unreliable in most cases.

So that the arc electrodes could be made to meet at a known instant and speed, a spring-loaded anode was designed and constructed, fig. 17. The anode was driven towards the cathode by a small compression spring, the movement being initiated by a trigger lever which was arranged so that the act of releasing the anode also broke an electrical contact and thus could be used to trigger the main timebase of the oscilloscope. Provided the electrode spacing was accurately set on drawing the arc, the time of impact was predictable and the timebase controls could be preset accordingly to give an expanded time scale at the right moment. The displacement transducer set up for previous voltage-length measurements proved very useful for setting the arc length to within a few %. This system proved quite reliable except at the fastest timebase speeds. Two designs of anode were used; for



movement of trigger lever  
releases spring-loaded anode  
and breaks electrical contact at \*

flexible  
connection  
to permit  
movement  
of anode

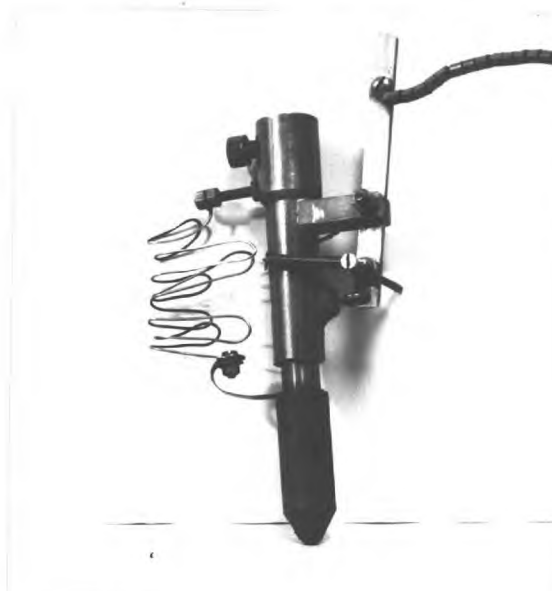
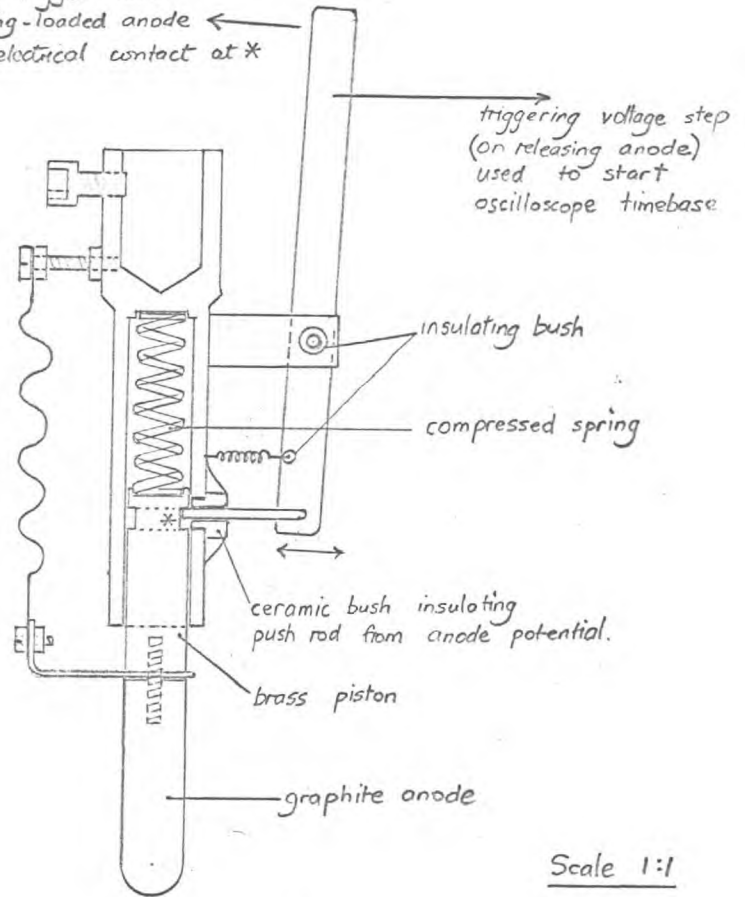


Fig 17. Spring-loaded anode A.

convenience these will be referred to as anode A and anode B.

Anode A, fig. 17, was the first one used. The spring and triggering mechanism were all inside the bell jar, being operated by a lever through a rotary seal in the baseplate. This device could be used at any gas pressure but suffered from overheating at large currents, causing it to stick.

Anode B, fig. 18, was water-cooled to its tip and the triggering mechanism was outside the arc chamber. An additional advantage was that it was unnecessary to set the electrode gap accurately for each reading, the spacing was set by adjusting the position of the cathode at the beginning of an experiment. The spring pressure was derived from bronze bellows, which also allowed relative movement between the anode and the arc chamber; this did not give such a uniform velocity versus gap relation as anode A. At first it was thought that this mechanism was unsuitable for use at reduced pressures since the spring force was then assisted by atmospheric pressure and the behaviour of the device was very violent. This was later successfully rectified by using an adjustable spring to restrain movement of the anode.

In both cases, initially, the triggering voltage for the oscilloscope time base was simply the arc anode voltage but spurious triggering due to voltage fluctuations at low arc currents necessitated isolating the triggering system completely from the anode voltage.

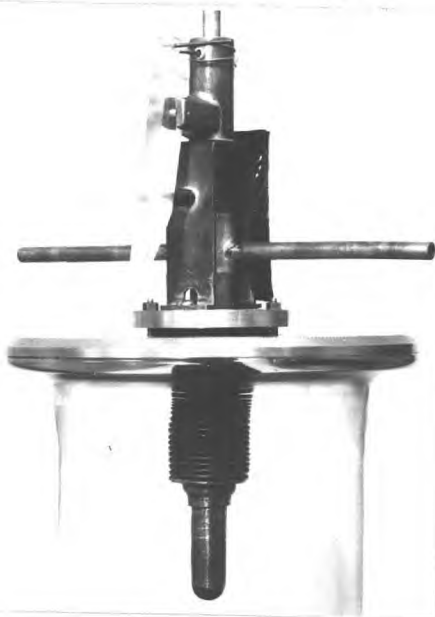
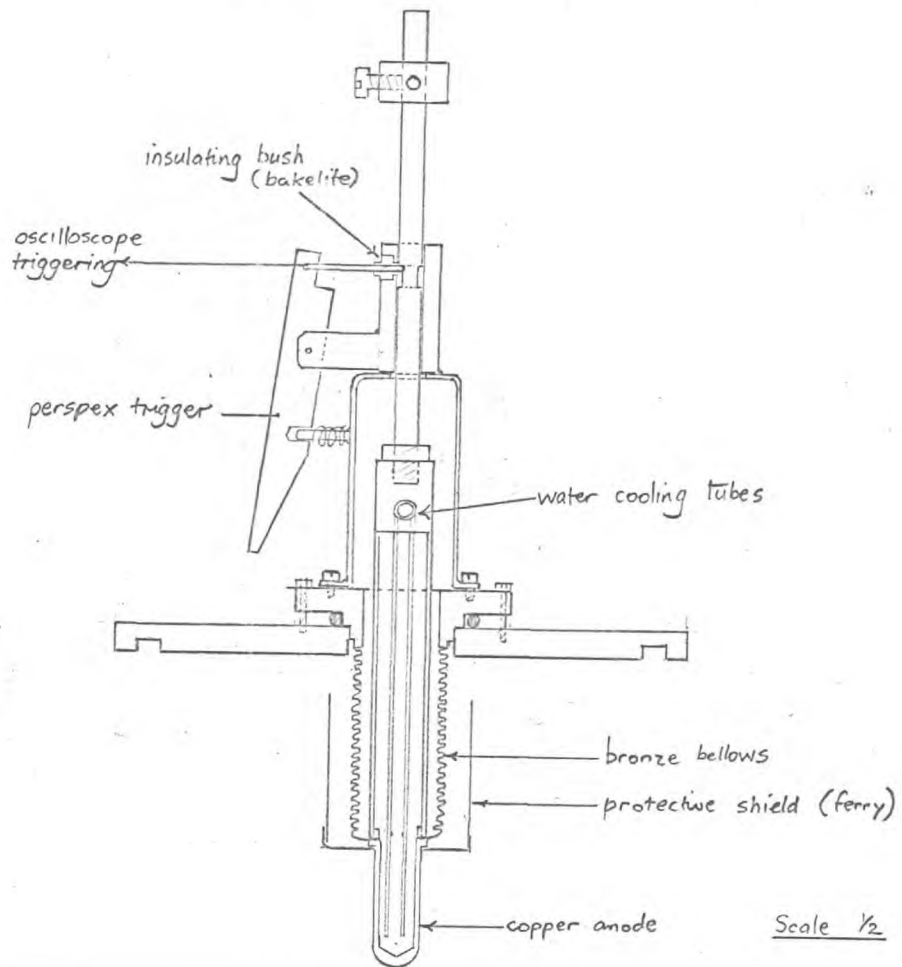


Fig 18. Spring-loaded anode B.

Anode A was clamped onto the water-cooled anode used in earlier experiments and the same arc tube was used. Anode B was built onto a brass flange and a new glass arc chamber made up consisting simply of a glass tube with a ground flange top and bottom. The vessels could be evacuated and gas-filled as in previous experiments.

For recording current, 'non-inductive' resistors of about 0.5 ohms were made. These were either bifilar, made by sawing a longitudinal slit in a carbon rod, or coaxial consisting of a carbon rod inside a brass tube, to which it was clamped at one end, the whole being cooled by blowing air between the rod and the tube. Since 80 volts of the total output of 100 volts were dropped across series resistors, small changes in arc voltage did not drastically alter the arc current.

#### 5.4. Measurement of Anode Velocity.

To obtain the maximum amount of information from the voltage versus time traces obtained by the above described method, it is necessary to know the velocity of the anode as it hits the cathode. This was obtained by measuring the time from triggering to contact as a function of electrode gap. The results are shown in fig. 19. The time was measured by applying 20 volts across the arc gap, with a series resistor to limit the short circuit current, and noting the position of the voltage step on the oscilloscope (which recorded the anode-cathode voltage) when the anode had been

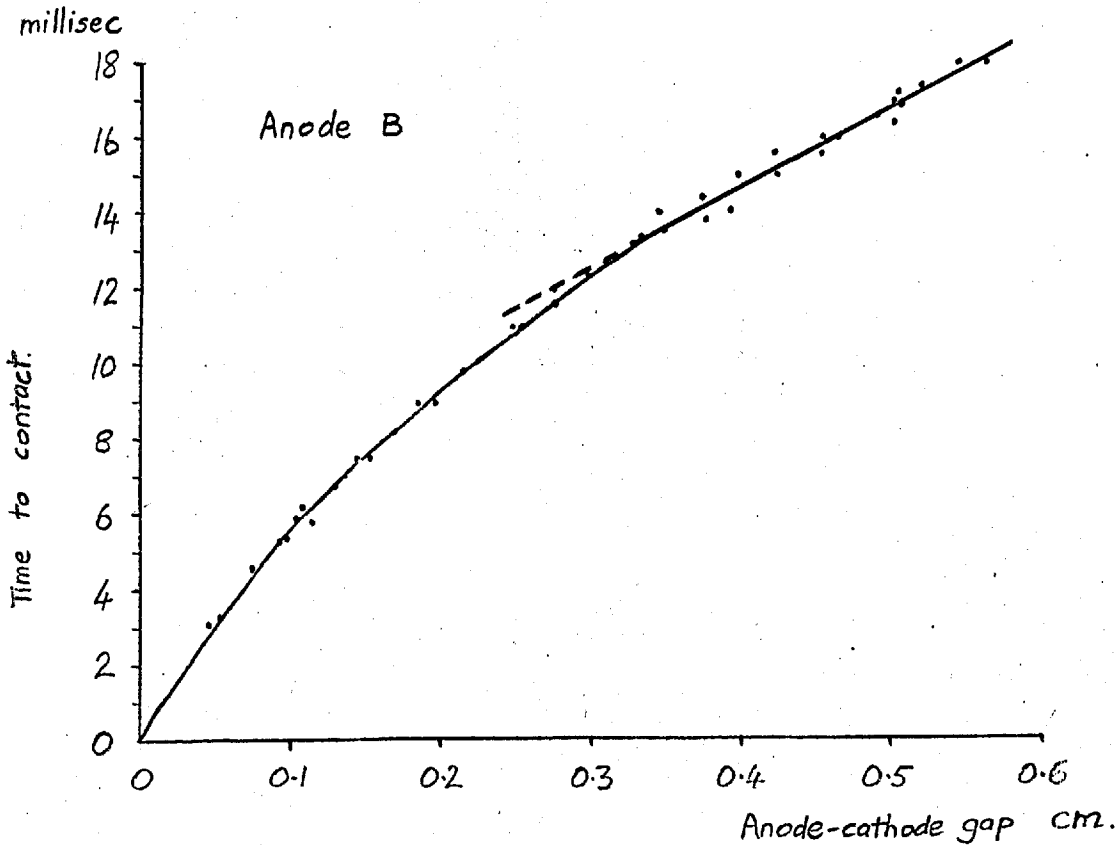
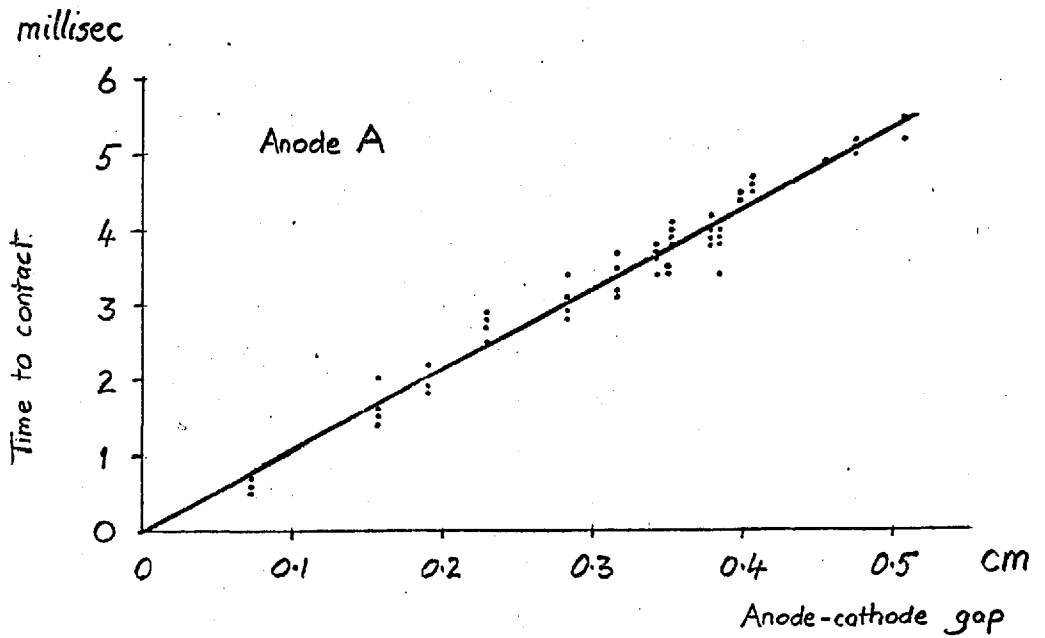


Fig 19. Speed calibration of spring anodes.

A: 92.5 cm/sec;      B: 47.2 cm/sec.

triggered. It is seen that anode A travels with effectively uniform velocity in the range of gaps 0.1 to 0.5 cm whereas anode B is accelerating, though the error in assuming uniform velocity in the range of interest, 0.3 to 0.5 cm, would not be large.

For anode A, the velocity is given by:

$$\frac{\text{initial electrode gap}}{\text{time from trig to contact}}$$

which makes allowance for different spring pressures easy. In the case shown, the velocity is 94 cm/sec. so that 1 millisecond on the oscillogram represents 0.094 cm of electrode gap. If 1 microsecond can be detected on the oscilloscope screen then in principle, distances of order  $10^{-4}$  cm can be measured.

Similarly, for anode B, at the spring pressure shown, the conversion is 1 millisecond represents 0.047 cm of electrode gap.

These anode velocities were somewhat arbitrarily chosen in the initial experiments but subsequent experiments with anodes of variable velocity showed that they were quite suitable.

## 5.5. Results with a tin cathode.

### 5.5.1. Cathode fall measurement.

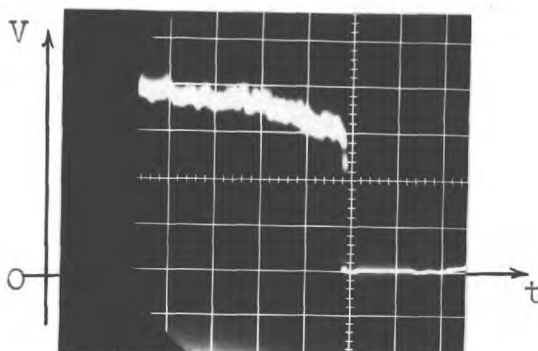
A high-purity graphite anode (A) and a U-tube dispenser cathode were set up in the glass arc chamber which was evacuated on the diffusion pump before being filled with dried argon to 760 torr. With the electrodes in contact, and the power supply delivering 100 volts, the series resistance was adjusted to give a

current of 10 amperes. An arc was drawn by separating the electrodes and the gap set accurately to 4 mm by the displacement transducer, its output being read off a chart recorder. The anode was then clamped in place by a suitable thumb screw. The single-sweep control of the oscilloscope was set, the camera shutter opened and the anode trigger released. A typical oscillogram obtained thus is shown in (a) of fig. 20. By using the delayed time base, the trace was expanded around the voltage step to produce the results shown in (b) and (c), showing that the abrupt voltage drop in (a) as the electrodes contact (and the arc extinguishes) is discontinuous, taking place in two steps.

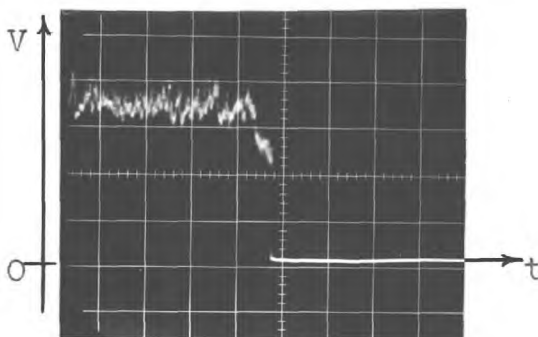
The anode took 5 milliseconds to travel 0.4 cm to the cathode so that as described above, 100 microseconds on the oscillograms represents 0.008 cm of anode-cathode gap. Referring to (c) of fig. 20, the arc voltage drops abruptly by  $\sim 5$  volts when the anode is  $\sim 0.003$  cm from the cathode; the voltage then decreases more slowly from 14 to 11 volts (with respect to the cathode) before dropping rapidly to zero as the electrodes touch. The distances over which the two abrupt potential drops take place are barely resolved, even at a scanning rate of 20  $\mu\text{sec}/\text{division}$ , so that the thickness of these regions must be less than about 1 microsecond.

When the anode is about  $3 \times 10^{-3}$  cm from the cathode, the arc voltage changes abruptly at a rate of  $5/10^{-6} = 5 \times 10^6$  volts/sec. and then, when the electrodes contact, the remaining voltage across the arc disappears at a rate of  $11/10^{-6} = 1.1 \times 10^7$  volts/sec. If

(a) 1000 microsec  
per division



(b) 100 microsec



(c) 20 microsec

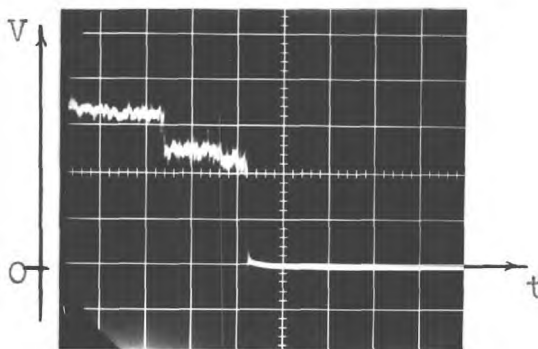


Fig 20. Oscillograms showing arc voltage versus time as the anode and cathode of an arc discharge are brought rapidly together, and the effect of expanding the time scale of the measurement around the moment of impact.

Tin cathode, graphite anode, argon, 760 torr.  
Current: 10 amperes.

Voltage scale: 5 volts/division.



it can be assumed that the electric fields close to the cathode and anode remain unchanged during the movement of the anode, then by taking into account the anode velocity of 80 cm/sec. along the arc axis, the time scale of the measurement may be replaced by a distance scale representing thickness in front of the electrodes. With this assumption, the oscillograms indicate the existence of two regions at, or close to, the electrode surfaces where the electric field is at least  $6 \times 10^4$  volts/cm and  $1.4 \times 10^5$  volts/cm respectively.

The question as to whether the fields have time to readjust themselves as the arc is shortened is equivalent to asking how long it takes the arc to assume a new equilibrium. When the anode-cathode gap is  $3 \times 10^{-3}$  cm the transit time for ions is of the order  $10^{-8}$  seconds, assuming they have thermal velocities in the range  $4 \times 10^4$  to  $10^5$  cm/sec. corresponding to gas temperatures in the range  $1000^\circ\text{K}$  to  $6000^\circ\text{K}$ . The anode takes 40  $\mu$  seconds to close this gap, i.e. about 1000 times longer, so that if it is assumed that the relaxation time is of the same order as the transit time (or even an order longer), there is ample time available for the discharge to become modified as the gap closes.

The anode is not behaving like a probe of fixed potential, but is actually part of the discharge, and free to adopt the potential demanded by the particular discharge conditions. While it may be argued that the mechanism in the anode and cathode regions may be greatly disturbed when the electrodes are very close together, the experimental results seem to suggest that this is not the case.

Any disturbance of the mechanisms near the electrodes would be expected to increase the voltage requirement there, but the voltages obtained are consistent with the indications of electrode fall obtained from voltage-length plots on long arcs. Since similar techniques have been used to find the cathode fall of glow discharges,<sup>39</sup> it seems reasonable to suppose that the rapid changes in arc potential as the electrodes approach one another represent, in voltage and thickness, the anode fall and cathode fall of the arc. The first step is believed to represent the anode fall ( $V_a = 5$  volts) and the final step the cathode fall ( $V_c = 11$  volts). The intervening region will be discussed later.

#### 5.5.2. Influence of Anode Material.

The choice of a different anode material may be expected to influence the size of the anode fall  $V_a$ , but it would be surprising if the cathode fall were altered also, unless sufficient anode material were evaporated to radically alter the whole arc behaviour.

Anode B was used, with various anode materials attached to the water-cooled copper by means of a copper sleeve with clamping screws. The anode details were as follows:

- (i) copper, water-cooled, 1/2" diameter, round tip;
- (ii) graphite: high-purity, 3/8" diameter, round tip;
- (iii) tungsten: 1/4" diameter rod, round tip;
- (iv) tin: porous stainless steel disc welded into a 3/8" o.d. stainless steel tube, and fed with tin from inside the tube.

The final potential drop as the electrodes touched was in all cases 11 volts, supporting the contention that this represents the cathode fall  $V_c$ . The height of the first step varied slightly with anode material, thus giving  $V_a$ . In all cases  $V_a$  and  $V_c$  were successfully separated over a range of currents (at least 10 to 30 amperes). The results are included in Table I.

### 5.5.3. Current Dependence.

With a tin cathode and graphite anode in argon at 760 torr,  $V_c$  and  $V_a$  were measured for currents in the range 3 - 60 amperes.  $V_c$  was found to be independent of current up to 25 amperes, fig. 21. In the range 25 to 60 amperes,  $V_c$  increases with increasing current. The deviation in  $V_c$  at any current is about  $\pm 1$  volt whereas  $V_a$  was found to vary rather more. The anode fall is apparently independent of current in the range 3 to 60 amperes.

Current measurements, using a 'non inductive' resistor of about 0.5 ohm in series with the arc showed that the current changed from 10 to 10.7 amperes when an anode fall of 5 volts disappeared, fig. 22. In view of how little the electrode falls change with current, it can safely be assumed that the current is constant as the electrodes are brought together.

### 5.5.4. Influence of ambient gas.

(1) Argon. Most of the experiments were carried out in argon since it is inert and monatomic. The voltage gradient in the arc column is also conveniently low.

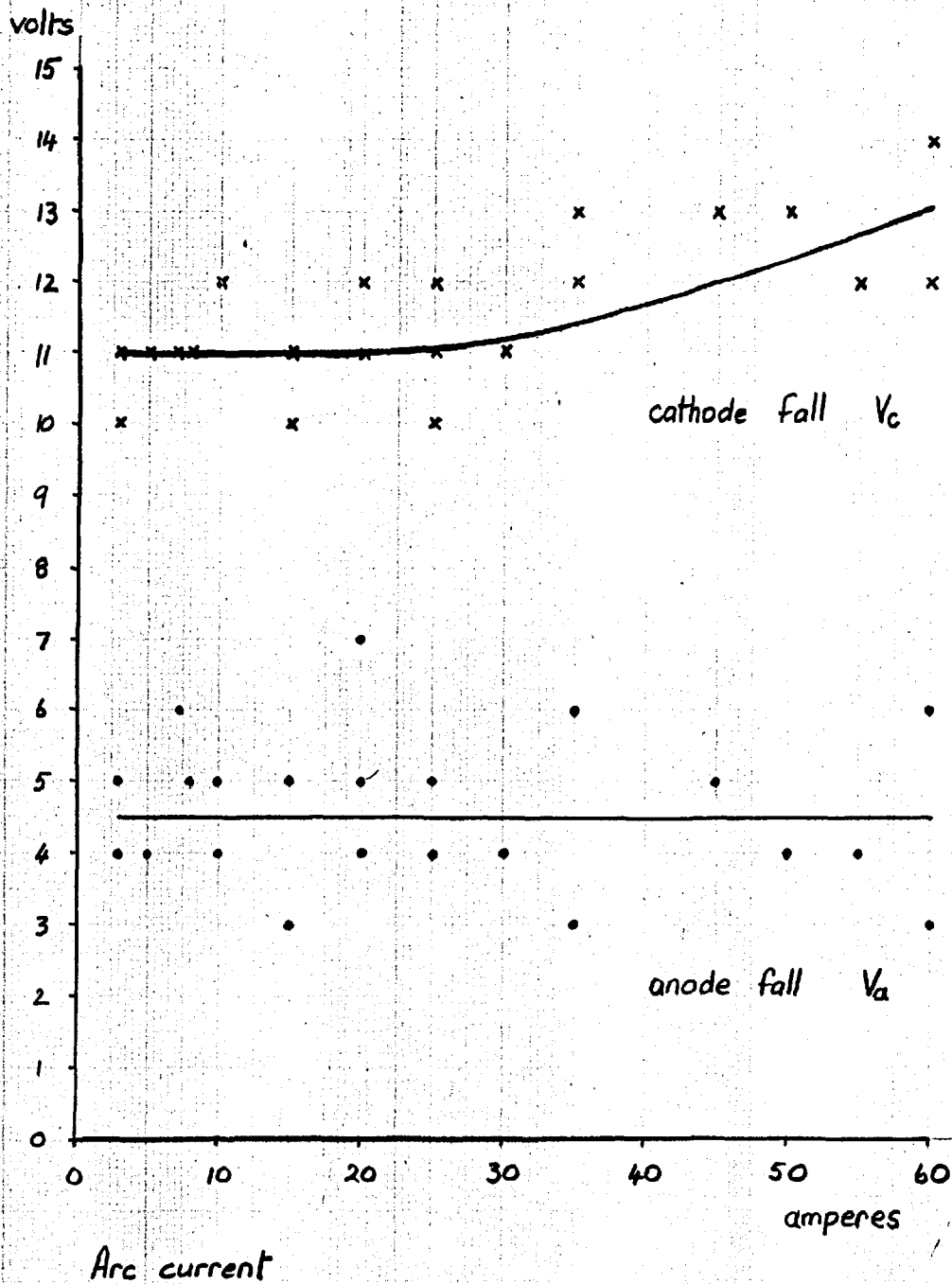


**Fig 21.** Current dependence of the cathode fall and anode fall.  
(Tin cathode, graphite anode, argon 760 torr).

The results may be summarised briefly thus:

$V_c = 11$  volts,

$V_a = 2$  to 5 volts, depending on anode material and/or geometry.

$V_a$  disappears abruptly when the anode-cathode gap is in the range  
 $1-5 \times 10^{-3}$  cm (see Chapter VI).

Electric field in the cathode fall space at least  $1.4 \times 10^5$  v/cm.

and in the anode fall space at least  $6 \times 10^4$  v/cm.

(2) Nitrogen. This was chosen to find the influence of a non-oxidising gas. 'Oxygen-free' nitrogen was used (British oxygen Company - 'white spot').

The apparatus and method were the same as those used for argon; the water-cooled copper anode (B) was used. Typical oscillograms are shown in fig.23. At anode-cathode contact, the voltage across the arc dropped abruptly to zero from 13 volts. When the oscilloscope time-base scale was expanded, the final 0.2 milliseconds of the trace was found to have a steeper slope than the preceding parts. Even at the fastest scanning rates, no voltage discontinuity was found, only this change in field; the final voltage drop was now 10 volts. This is interpreted as follows.

The final drop of 10 volts gives the cathode fall  $V_c$ . The drop from 13 volts to 10 volts immediately preceding the disappearance of the cathode fall, represents the anode fall of 3 volts spread over a thickness of 0.2 milliseconds =  $7 \times 10^{-3}$  cm, since the anode speed was 35 cm/sec. The field in the anode region is therefore  $3/(7 \times 10^{-3}) = 400$  volts/cm. The thickness of the cathode

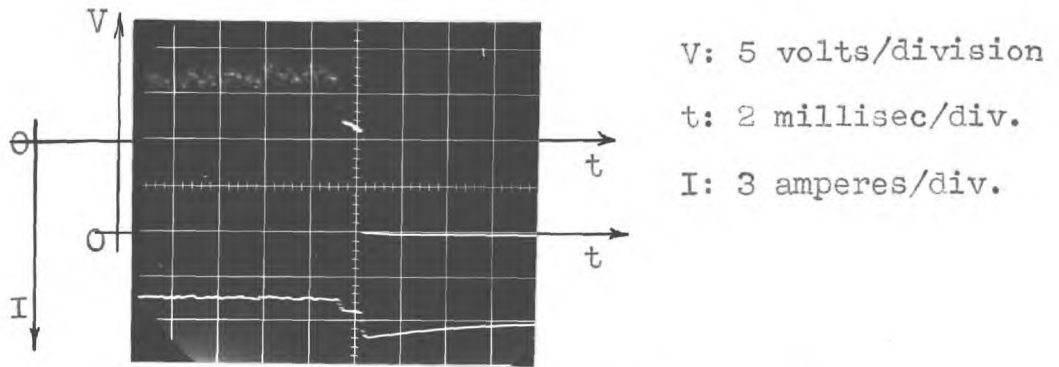


Fig 22. Variation of arc current at contact.  
Tin cathode, graphite anode, argon.

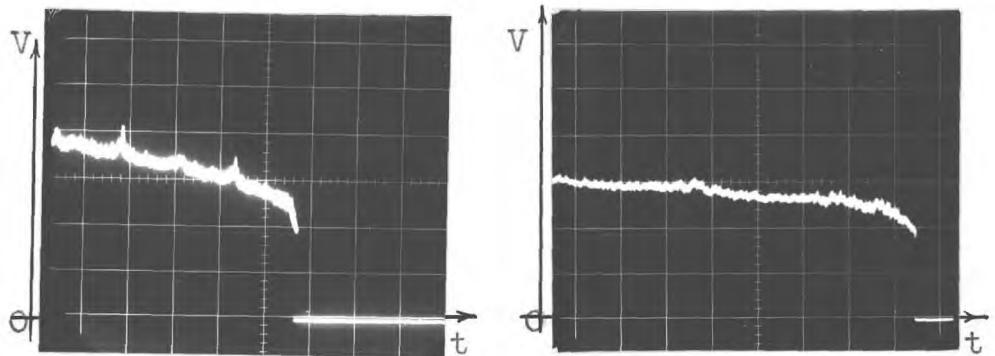


Fig 23. Electrode drop of tin cathode in nitrogen at  
760 torr. Anode: cooled copper. 10 amperes.

region was not resolved and must be of the same order as when argon was the ambient gas.

#### 5.5.5. Pressure Dependence.

Using the same apparatus and method as above it was possible to study the arc over a wide range of ambient gas pressures below atmospheric. The arc chamber was first evacuated, and then filled to the desired pressure with the appropriate gas.

(1) Argon. In the pressure range 100 to 760 torr, very little change in the arc appearance or voltage occurs. As the pressure is further reduced, the column becomes more diffuse and stable until a pressure of about 1 torr, when the arc will probably extinguish.

Electrode drop measurements carried out at 50 torr intervals from 1 to 760 torr detected no variation in either  $V_c$  or  $V_a$ .

(2) Nitrogen. The cathode fall  $V_c$  was found to be independent of ambient nitrogen pressure in the range 5 to 760 torr. The anode fall  $V_a$  increased at low pressure, being 8-10 volts in the range 5-80 torr compared with 3 volts at high pressure.

Typical oscillograms at a low ambient pressure of nitrogen are shown in fig.24. These show two voltage steps, similar to those found in high pressure argon except that the anode fall comes and goes a number of times before finally disappearing. This effect is greater, the lower the ambient gas pressure. This can probably be accounted for by the diffuse nature of the arc column at low

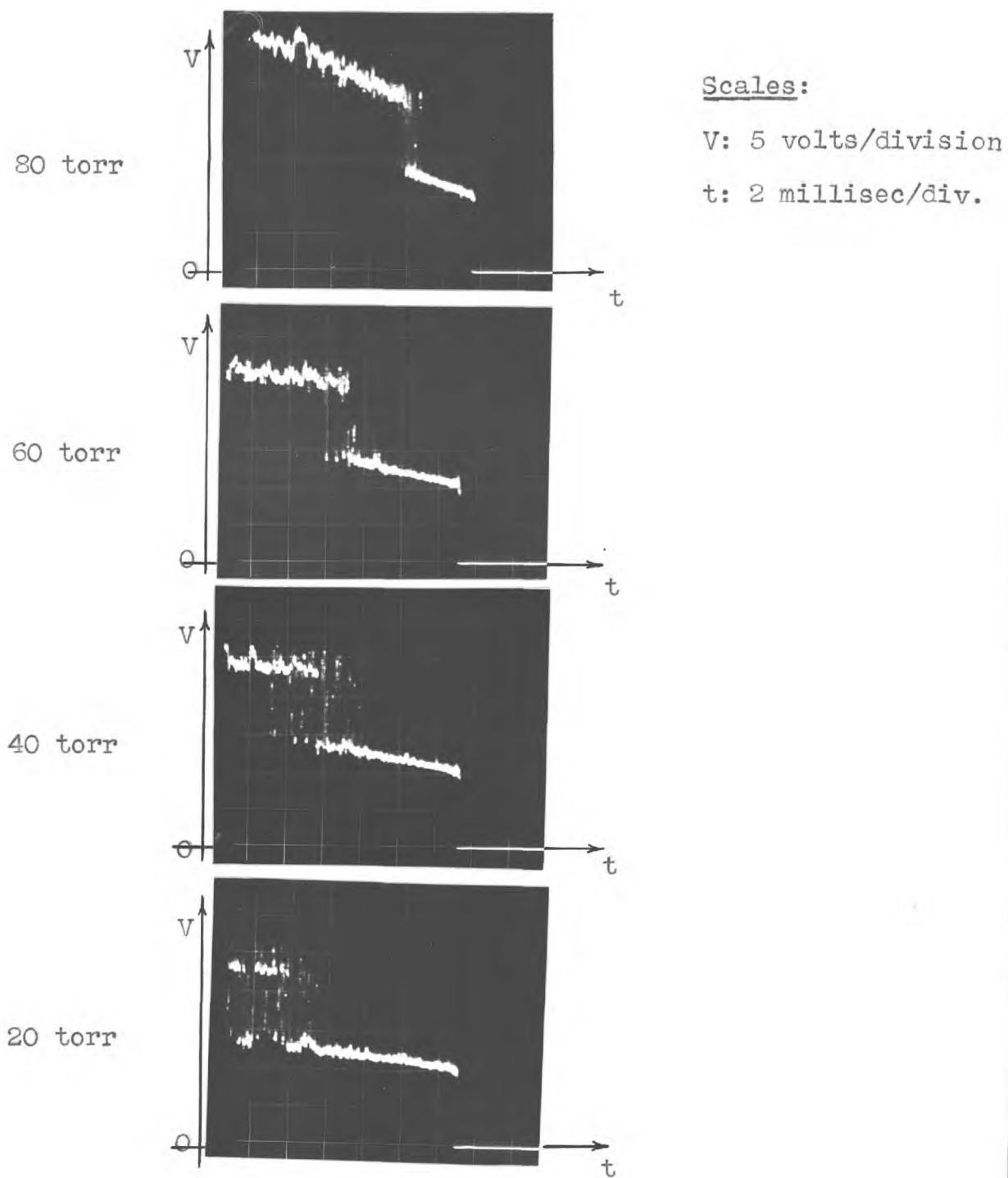


Fig 24. Cathode fall and anode fall for a tin cathode, copper anode, 10 ampere arc in nitrogen at reduced pressure.



pressures, resulting in the column diameter being often greater than the diameter of the electrodes.

The cathode fall  $V_c$  was found to increase with current at low pressures. The results at an ambient nitrogen pressure of 80 torr are given in fig.25. An increase in  $V_c$  of approximately 1 volt per 10 amperes increase in arc current was found in the range 10 to 40 amperes.

A tin pool cathode in low pressure nitrogen gave virtually identical results to those described above for the dispenser cathode.

#### 5.5.6. Conclusion.

The technique by which the above results were obtained represents a new, and powerful, method of studying arc discharges. It has been possible to measure the cathode fall and the anode fall of an arc with a tin cathode under a wide range of conditions. For comparison and fundamental interest, it seemed desirable to make measurements on other cathodes, using the same method. The results of these further investigations are given below.

#### 5.6. Results with a graphite cathode.

##### 5.6.1. Introduction.

The arc with carbon (or graphite) electrodes is a specially interesting case to study, since depending on the nature and pressure of the ambient gas, the current and the electrode geometry, the arc may have a thermionic or a vapour cathode spot. This can also be observed with other 'normally' thermionic cathode materials.

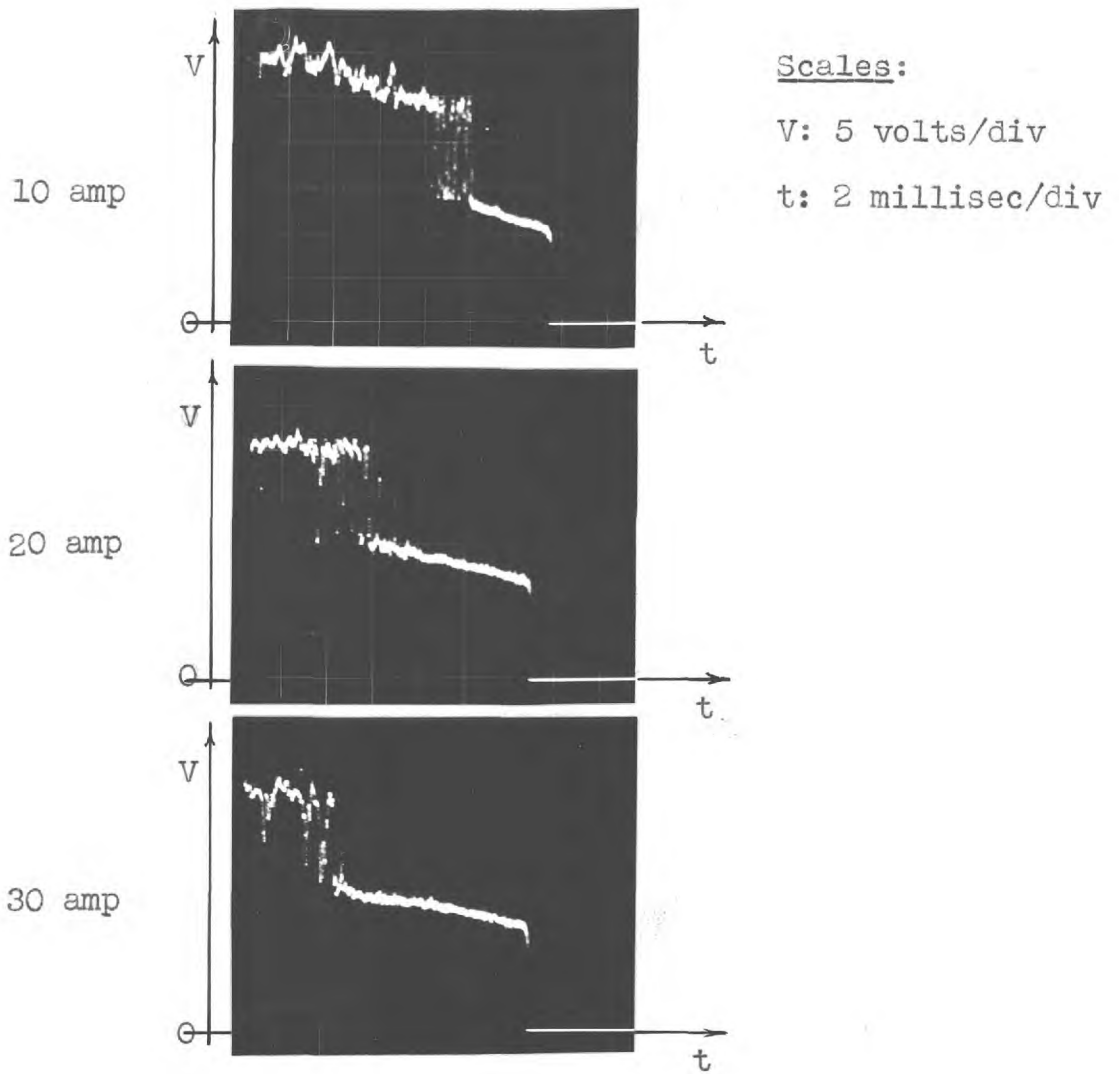


Fig 25. Variation of cathode fall with current at low pressure. (Tin cathode, copper anode, nitrogen, 80 torr)

Which type of cathode behaviour occurs in any case has been expressed by von Engel and Arnold<sup>40</sup> as depending on "whether intense evaporation of, or thermionic emission from, the cathode spot occurs on starting the arc, as the spot temperature rises".

This behaviour can be explained by assuming that the vapour cathode spot is maintained by excited atoms<sup>13</sup> which release electrons from the cathode, providing the excitation energy is greater than the work function. It is well known<sup>41</sup> that resonance radiation can be reduced in intensity by the presence of a foreign gas. This is attributed to the destruction of excited atoms by a process known as 'quenching'. Although various mechanisms can account for quenching, depending on each particular case, it is generally found that molecular gases, and in particular hydrogen, show strong quenching and the rare gases helium, neon and argon show little or no quenching. It is found that the rare gases usually support vapour arc spots, and that in molecular gases the thermionic arc spot will often change to a vapour spot as the ambient pressure is reduced. Thus a thermionic spot is to be expected if the concentration of atoms or molecules capable of quenching excited atoms is sufficient in the cathode region to starve the cathode of excited species capable of releasing electrons. Naturally, if the cathode is then incapable of supplying sufficient electrons by thermionic emission the arc will extinguish.

### 5.6.2. The Graphite Arc in Argon.

The first experiments were carried out with electrodes of  $\frac{1}{2}$ " diameter high-purity graphite rod, having rounded conical tips. Argon was used to reduce electrode wear to a minimum and because it gave a stable arc, with a vapour type spot. Attempts were made to measure  $V_c$  and  $V_a$  by the method described above.

A typical oscillogram is shown in (a) of fig.26. It is seen that in the last 0.3 milliseconds (0.02 cm) before contact the arc voltage increases by 4 volts before dropping rapidly to zero in the usual way. This does not enable the cathode fall and anode fall to be separated, in fact it even casts some doubt as to the value of their sum. A possible explanation of this increase in arc voltage at short gaps is the existence of a minimum arc length, suggested by Bauer and Schulz<sup>42</sup> to be of the order 0.1 mm, with the result that if the electrodes are moved closer together than this, the arc moves to other parts of the electrodes where its length can be greater than the gap. The arc is effectively squeezed from between the electrodes. Alternatively the anode fall may be negative.

It was thought that this might be clarified by altering the electrode geometry. (b) and (c) of fig.26 show oscillograms obtained with a round anode and plane cathode, and a round anode and hollow cathode such that the anode fitted snugly into it, respectively. All show a rise before the final voltage drop, but the rise takes various forms; the cause of the rise is still in doubt.

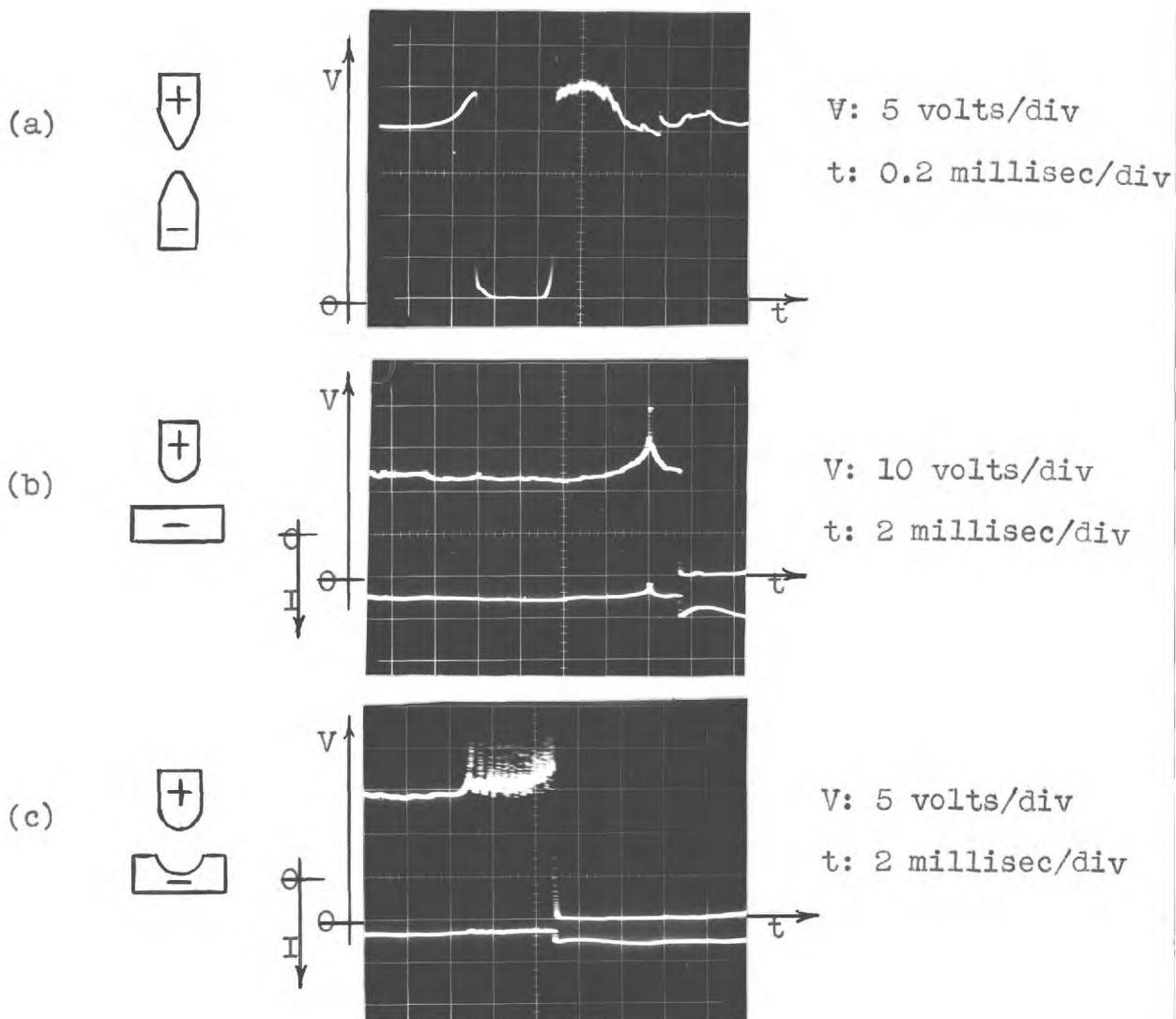


Fig 26. Electrode fall for graphite electrodes of different shapes, in argon at 760 torr. Current: 10 amperes. (Lower trace is current measured downwards from centre line).

When the timebase scanning rate was increased to 200  $\mu$ sec, 50  $\mu$ sec, and finally 10  $\mu$ sec per division, no further discontinuity was found.

### 5.6.3. The Graphite Arc in Air.

Since, in general, argon supports a vapour cathode spot and air a thermionic one, it should be possible to observe a transition from one to the other if the proportion of air to argon in a mixture of the two gases is gradually increased. With the sphere to plane geometry used in the above experiments, electrode drop measurements were carried out in mixtures of argon and air.

A large proportion (probably about 50%) of air had to be added to the argon before the rise before the final drop described above ceased to be observed. But even small proportions of air influenced the voltage level before this final rise. In pure argon it was 21 volts, but with 2 $\frac{1}{2}$ % air it decreased to 15 volts and then rose again to its former value by the time 20% air had been added. In 100% air, the final voltage drop at contact was 15 volts and speeding up the oscilloscope time scale produced no discontinuity. The conclusion to be drawn from these results is that the rise in voltage at short gaps is a property of certain types of vapour arcs. The electrode potential fall of a graphite arc in air appeared to be a function of the initial arc length, being greater for shorter arcs; it was usually about 15-25 volts.

The transition from a thermionic to a vapour type cathode should be observed if the ambient air pressure around a carbon arc

in air is reduced. The results of doing this are given in fig.27. The hollow cathode was used in these experiments, but similar results were observed with other geometries. The relatively smooth trace at atmospheric pressure, showing a voltage drop of 25 volts in this case, started to show irregularities at an ambient air pressure of about 150 torr, and when the pressure had been reduced to 50 torr and below, a distinct step appeared in the trace. This was accompanied by typical cold cathode behaviour, in that the relatively large stationary thermionic cathode spot contracted and became more mobile, while carbon was deposited on the inside of the glass arc chamber. The trace at below 150 torr shows the characteristic rise before the electrode fall observed in argon, but in this case the anode fall  $V_a$  and the cathode fall  $V_c$  are separated, having the values  $V_c = 18$  volts and  $V_a = 5-8$  volts.

#### 5.6.4. Summary of Carbon Arc Measurements

At the outset, it should be pointed out that graphite is an unusual material as regards its behaviour on heating, its melting and vaporisation behaviour is expected to be different to that of metals.

It has been verified that the cathode spot on a graphite electrode can behave in different manners, depending on the ambient gas and its pressure. For convenience these will be referred to as vapour and thermionic modes respectively.

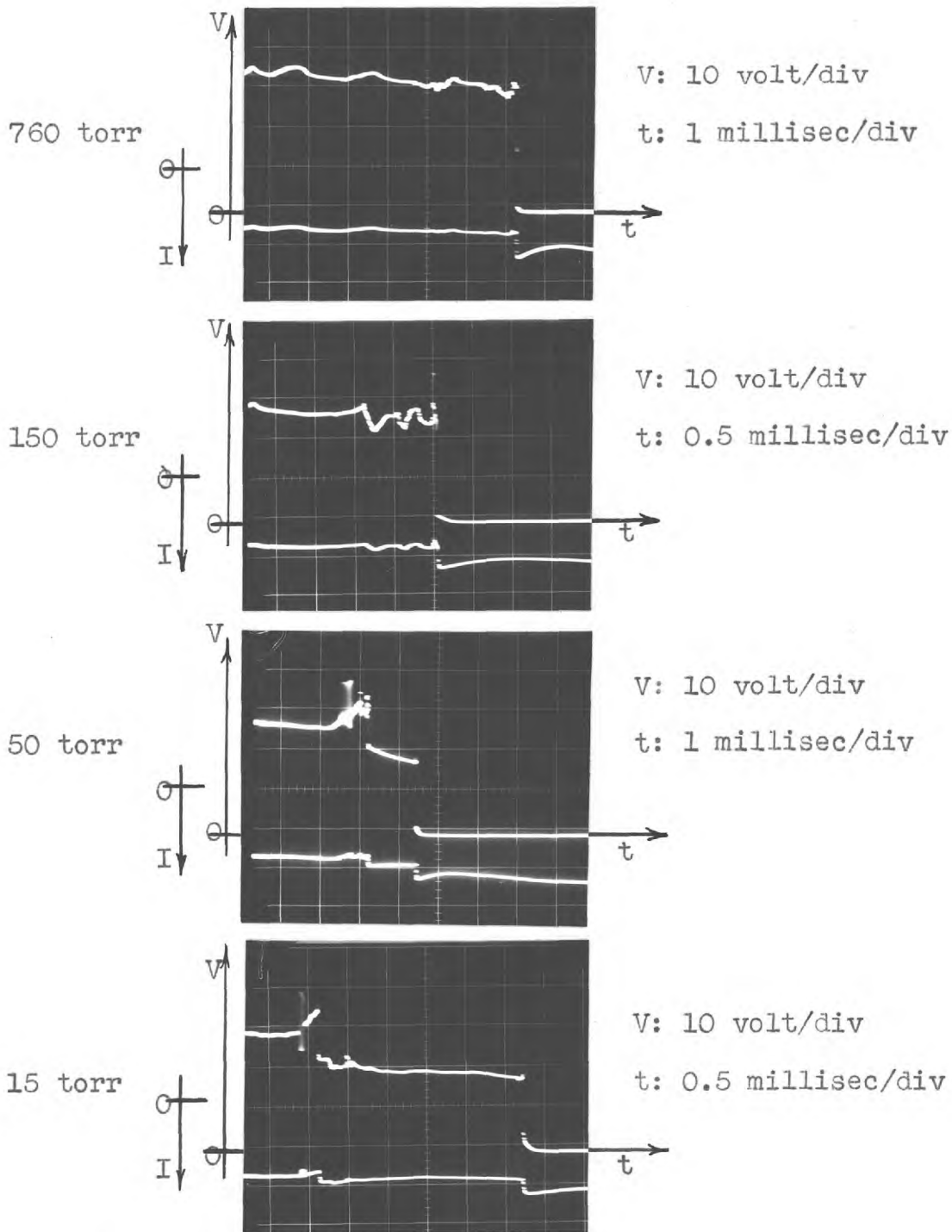


Fig 27. Electrode potential fall of a graphite arc in air as the ambient pressure is reduced. Current: 10 amperes. (Lower trace is current, measured downwards from centre line).



It has not proved possible to separate the cathode fall and the anode fall of the graphite vapour arc burning at atmospheric pressure owing to the erratic and large increase in total arc voltage occurring at electrode spacings of the order 0.2 mm. This feature does however appear to be characteristic of the vapour mode, as it is absent when sufficient air has been added to the ambient gas to produce a thermionic arc.

The transition from thermionic mode to vapour mode on reducing the ambient air pressure has been observed, and the cathode fall and anode fall of the vapour mode arc at low pressure have been measured.

#### 5.7. Results with other Electrode Materials.

##### 5.7.1. Copper.

The cathode spot on copper is generally believed to be of the vapour type, results similar to the tin measurements are therefore to be expected.

At low currents, the anode region appeared to be extended resulting in a change in slope rather than a voltage step as the anode fall disappeared. This makes the anode fall rather indeterminate as, in the oscillograms, it merges with the positive column which at these short gaps has a fairly high gradient anyway. The cathode fall was 12-14 volts for a 10 ampere arc, the anode fall 5 volts spread over 0.25 mm, giving an anode field of  $5/0.025 = 200$  volts/cm.

When the current was increased to 30 amperes, oscillograms resembling the tin ones were obtained with two abrupt steps but showing higher cathode fall and anode fall of  $V_c = 20$  volts and  $V_a = 10$  volts. In this case the anode fall thickness was very small.

The above results are in argon at 760 torr; in atmospheric pressure nitrogen the arc was too erratic to permit useful measurements but when the pressure was reduced to below 150 torr a stable symmetrical arc was obtained. The traces of arc voltage against electrode gap were very similar to those obtained with a tin cathode at low pressures. The anode fall tended to disappear a number of times before finally going and the cathode fall  $V_c = 16$  volts and anode fall  $V_a = 10$  volts were independent of pressure in the range 60 to 150 torr, and independent of current in the range 7 to 45 amperes.  $V_a$  has the same value as obtained under similar conditions when a tin cathode was being used.

#### 5.7.2. Tungsten.

Being a high melting point metal, tungsten is expected to exhibit thermionic or vapour cathode spots depending on the conditions, in much the same way as graphite does.

The arc in air at atmospheric pressure with 1/4" diameter tungsten electrodes (rounded and polished) gave a very smooth voltage versus gap trace which dropped to zero from 20-25 volts. This abrupt drop could not be resolved further, but this may have been due to the oxide which quickly built up on the cathode

and prevented 'clean' contact. The voltage gradient just before the final drop was about 100 volts/cm.

In argon with just enough air to stabilise the arc, its behaviour was vapour type. The trace then showed fluctuations of the nature typical of such an arc. The anode fall was not abrupt, and the results for a 10 ampere arc were  $V_c = 15$  volts and  $V_a \sim 5$  volts.

5.8. Discussion of Measurements of  $V_c$  and  $V_a$ .

The results are summarised in Table I.

(1) The Cathode Fall.

The cathode fall is seen to be characteristic of the cathode material and very little influenced by the ambient gas. The following have been established:

$V_c$ for tin	11 volts
copper	12 volts
tungsten	15 volts (vapour mode).

Other relevant data are as follows:

	$\phi$	$V_i$	$V_{res}$
Tin	$\sim 4.3$	7.3	4.33
Copper	4.5	7.7	3.78
Tungsten	4.4	8.0	2.3
Carbon	4.4	11.3	7.5

TABLE I

SUMMARY OF  $V_c$  AND  $V_a$  MEASUREMENTS

Cathode	Anode	Gas	P	I	$V_c$	$V_a$
Tin	Tin	A	760	10	11	2
"	Tungsten	A	"	"	11	3
"	Copper	A	"	"	11	4
"	Graphite	A	"	"	11	4-5
"	"	A	"	60	13	4-5
"	Copper	N <sub>2</sub>	"	10	10	3
"	"	N <sub>2</sub>	10-80	"	10	8-10
"	"	N <sub>2</sub>	80	30	13	10
Copper	Copper	A	760	10	12-14	~5
"	"	A	"	30	16-20	8-10
"	"	N <sub>2</sub>	60-150	10	16	10
"	Graphite	A <sup>2</sup>	760	10	12	1-5
Graphite	Graphite	A	760	10	Sum	15-25
"	"	air	760	"	"	15-25
"	"	air	50	"	18	5-8
Tungsten	Tungsten	A	760	10	15	~5
"	"	air	"	"	Sum	20-25

Assuming that the emission of electrons is due to the impact of excited atoms, excited atoms with energies lower than the work function  $\phi$  are 'wasted' as far as electron emission is concerned, though they may assist in vaporisation<sup>43</sup>. The result of this is that where there are atoms of low excitation energy the cathode fall is likely to be higher than otherwise.

The most studied cold cathode arc is mercury. The cathode fall is 8 volts (as measured by previous techniques),  $\phi = 4.5$  volts,  $V_{res} = 4.9$  (then 6.7). All the excited states have energies greater than the work function.

Comparing these figures with those given above it is seen that the work function of tin is almost identical to the first excitation potential (Landolt-Bernstein Tables, 1955, give  $\phi$  varying between 4.2 and 4.4 with a most likely value of 4.39) and from the measured cathode fall, compared with mercury, it would seem probable the excited atoms of energy 4.33 volts are incapable of releasing electrons from the cathode. The cathode fall of copper can be explained in a similar way; the wastage of excited states with energies lower than  $\phi$  gives a higher cathode fall than on mercury, even though the work function and resonance potential are quite similar. The same reasoning can be applied to the tungsten cathode.

(2) The Anode Fall.

The anode fall was found to be more variable in magnitude and thickness than the cathode fall. The anode fall arises from the excess negative space charge at the anode surface owing to its positive potential and the fact that it does not normally emit ions.

A consideration of the energy balance may explain why the results were so variable. The energy gained by the anode is represented by the kinetic energy and potential energy of the electrons and by the thermal (and also excitation and chemical) energy of the gas atoms, and energy is lost by evaporation, radiation and conduction<sup>14</sup>. Thus the energy balance, per ampere of electron current, may be expressed as

$$V_a + \phi + V_{\text{therm}} = V_{\text{cond}} + V_{\text{evap}} + V_{\text{rad}}$$

so that the anode fall depends on a number of variable quantities, which would have to be controlled more carefully in a detailed study of the anode region.

Also, the conditions in the anode region may not be as simple as assumed here, e.g. reflection of positive ions and excited atoms is a possibility if they arrive in large numbers owing to the proximity of the cathode region when the arc is very short.

In most cases the anode fall thickness was less than  $10^{-4}$  cm, which was the case in all the tin experiments carried out in argon. Sometimes no abrupt voltage step marked the disappearance of the anode fall, the voltage-gap trace simply became steeper when the

anode was very close to the cathode; this can mean either that the anode fall disappears slowly as the electrodes meet, or that the anode fall thickness itself is fairly large. In some instances it may be that the anode fall is zero. The anode fall thickness seemed to depend on the nature of the cathode, but this may be due to the initial arc length being usually only 3 to 4 mm, considerable cathode material being evaporated and since the arcs were initiated by separating the electrodes all combining to give a high probability of cathode material adhering to the anode surface.

The results may be summarised thus:

<u>Anode fall thickness.</u>	<u>Conditions.</u>
$< 10^{-4}$	Strongly evaporating cathodes. Usually marked voltage fluctuations.
$\sim 10^{-2}$	Cooled copper anode, except when cathode evaporating strongly.
merging with column	Arcs with high melting point electrodes, operating in thermionic mode.
? see fig.26	Graphite electrodes in argon.

When the anode and cathode are of different metals, there will exist a contact potential difference between them, when they are separated, equal to the difference in the work functions. From the table in section 5.8 it is seen that the work functions of the metals used are within 0.2 volts of each other; accordingly the contact difference of potential has been neglected.

CHAPTER VI.

THICKNESS OF THE CATHODE REGION.

6.1. Definition of the cathode region.

In the previous chapter, it was pointed out that as the anode-cathode gap of an arc is rapidly closed the anode fall and cathode fall show themselves as steps in the voltage versus time (or distance) plot. It was also pointed out that the disappearance of the cathode fall takes place a short interval in space and time after the disappearance of the anode fall. This is clear in fig.20. This discussion applies to the vapour arc. The anode and cathode fall usually occupy thicknesses of less than  $10^{-4}$  cm. In the vapour arc copious evaporation of cathode material takes place, this results in a high local vapour pressure in front of the cathode, which may extend to greater distances from the cathode than the cathode fall thickness. The region in front of the cathode where the vapour density is significantly above that in the arc column will be referred to as the 'cathode region'. It is believed that the part of the trace in the oscillograms between the anode fall and the cathode fall represents this region, since the potential there is only slightly above cathode fall potential.

The high vapour density is maintained by back-scattering of evaporated atoms by positive ions accelerated in the cathode fall<sup>14</sup>. This implies that the ions make many collisions in the cathode fall space, i.e. the ion mean free path is smaller than the thickness of the cathode fall. The result of this is that the number of atoms leaving the cathode surface is much greater than the number



escaping completely - the experimentally measured evaporation rate. Consequently, cathode temperatures estimated from the measured rate of evaporation are too low.

Outside the very strong field of the cathode fall thickness, back-scattering will be absent and the vapour density will fall off by diffusion. Robson<sup>44</sup> has shown theoretically that at distances of the order of a spot radius, the vapour density falls off very rapidly, reaching ambient at about ten spot radii. If the spot current density is  $10^6$  amperes/cm<sup>2</sup>,<sup>45</sup> then a 10 ampere circular spot would have a radius of  $1.8 \times 10^{-3}$  cm, so that at a distance of  $2 \times 10^{-2}$  cm in front of the cathode, the vapour density is expected to have fallen to ambient.

The results of cathode thickness measurements are given below.

## 6.2. Method.

The apparatus was identical to that used in the previous chapter for separation of the anode and cathode falls. Measurement of the anode speed and details of the relation between the oscilloscope timescale and distance between the electrodes has been given in 5.4 and fig.19.

## 6.3. The Cathode Region Thickness of the Tin Arc.

In all the oscillograms showing separation of the cathode fall and anode fall it is possible to estimate the thickness of the cathode region, but to obtain the greatest accuracy a fast time scale on the

oscilloscope should be used. A series of results with this aim were obtained, using a tin dispenser cathode and graphite anode in argon at 760 torr. The time scale was 20  $\mu\text{sec}/\text{division}$  so that each large division (cm) on the oscilloscope screen represented  $1.6 \times 10^{-3}$  cm (anode A, velocity 80 cm/sec.). The fifteen measurements are summarised in fig.28. For a 10 ampere arc, the most commonly occurring value was  $2.5 \times 10^{-3}$  cm, with over 90% of values lying within  $2 \times 10^{-3}$  cm of this.

This is remarkably close to the predicted value.

#### 6.4. Current Dependence.

The cathode region thickness was found to increase with increasing current as shown in fig.29. A threefold increase was found in the range 10 to 60 amperes.

#### 6.5. Influence of Ambient Gas Pressure.

At reduced pressure, the cathode region thickness is greater, and the boundary between it and the anode fall space is much more diffuse, as indicated in Section 5.5.5.

The thickness is then measured in millimetres, and may reach the whole distance to the anode, see fig.30. This greatly extended cathode region is found only below about 100 torr ambient gas pressure.

This thickness increases with increasing total arc current, twofold in the range 10 to 40 amperes.

Individual results in units of  $10^{-3}$ cm:

2.9 2.6 4.6 1.1 1.8 7.7 0.6 4.6  
2.2 3.4 2.6 2.9 4.5 1.6 2.2

Modal value:  $2.5 \times 10^{-3}$ cm

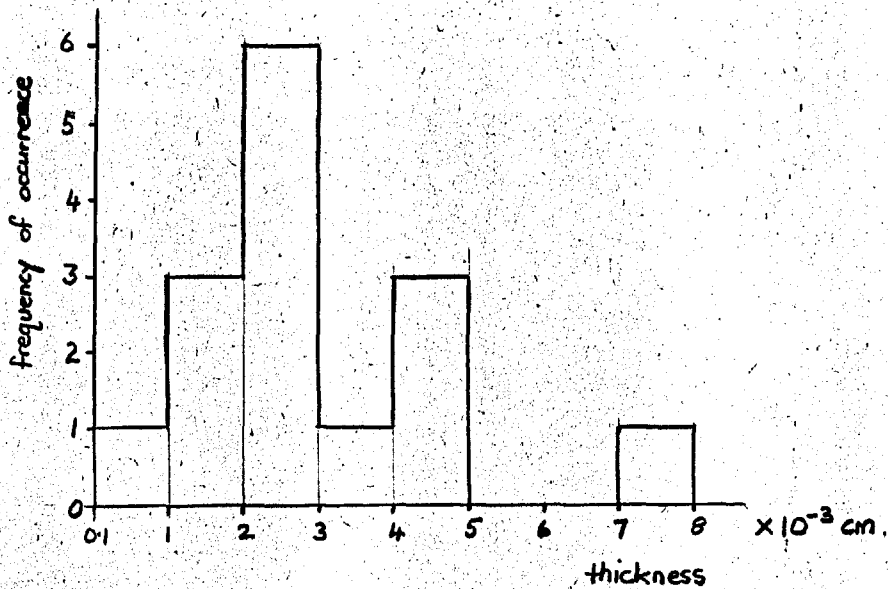


Fig 28. Cathode region thickness in front of a tin dispenser cathode. 10 ampere arc in atmospheric pressure argon, graphite anode.

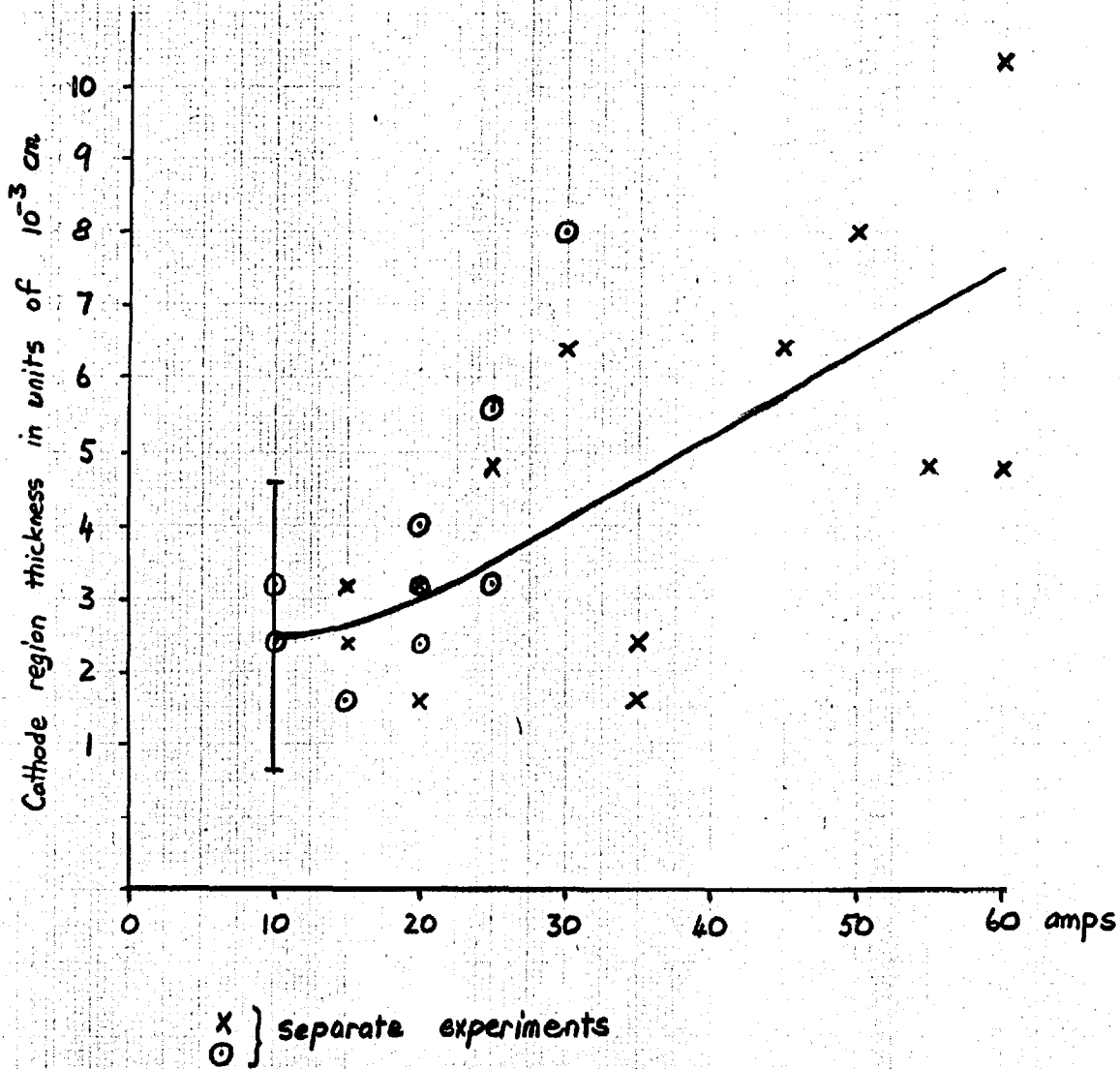


Fig 29. Current dependence of cathode region thickness. (Tin cathode, graphite anode, argon 760 torr).

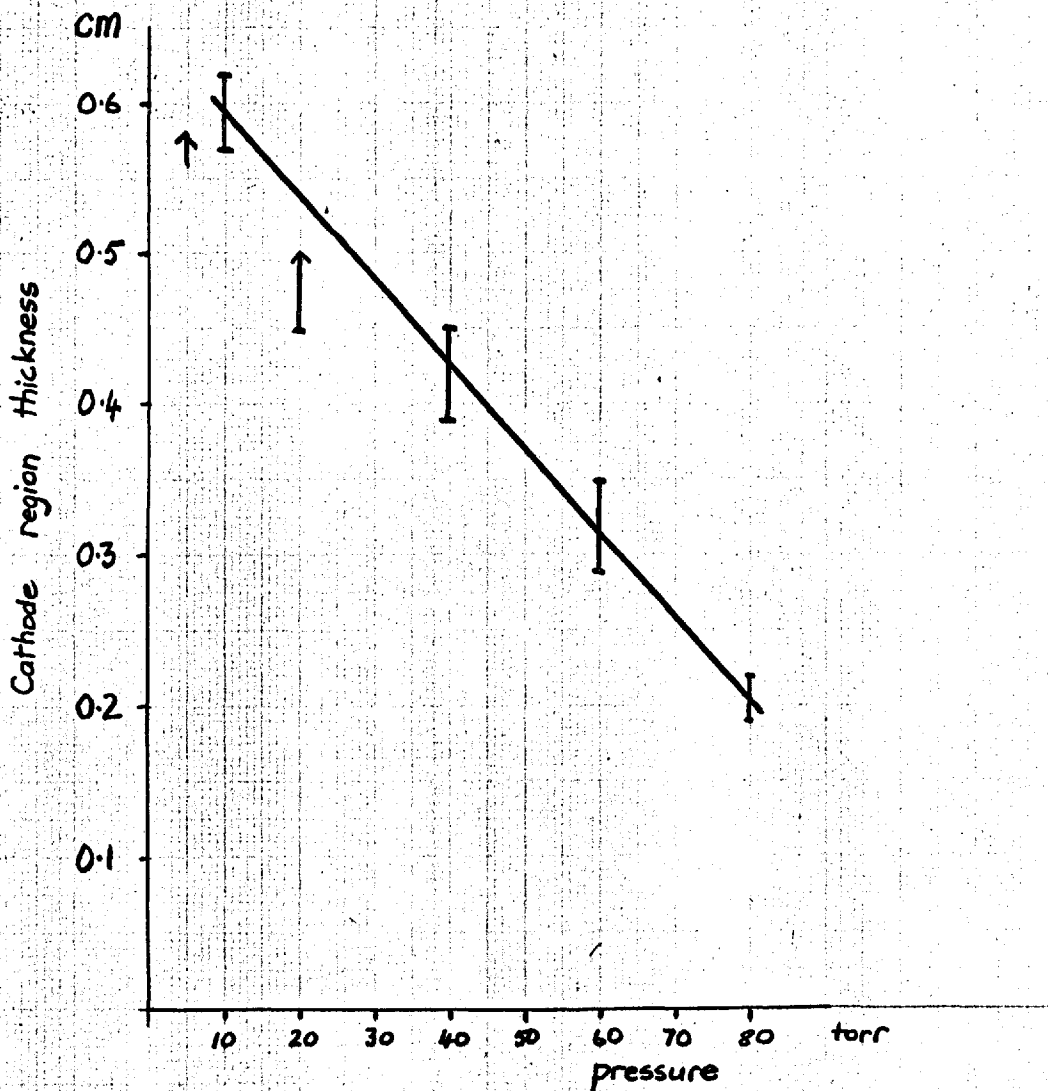


Fig 30. Thickness of the cathode region at low pressure. (Tin cathode, copper anode, nitrogen, 10 amp).

## 6.6. Interpretation of Oscillograms at Low Pressures.

In view of the large thickness of the so-called cathode region at low pressures and the calculations of Robson referred to above, it seems pertinent to ask whether the interpretation of this part of the trace at low pressure as representing a region of enhanced vapour density is reasonable. Reference to figs. 24 and 25 shows that the cathode fall thickness is still of the same order as at higher pressures - less than  $10^{-4}$  cm. Since the cathode fall is still only 10 volts, the cathode mechanism is that of the arc and not of the glow discharge, which requires a much higher cathode fall. The anode fall of 8-10 volts is higher than that obtained at atmospheric pressures, and so the mechanism there could be that of the glow discharge; the anode fall spaces of the glow and arc discharges are broadly similar, except that the temperature and current density in the latter are higher and the potential drop slightly lower.

The region on the traces between the anode and cathode falls is sharp at the cathode end and diffuse towards the anode; the electric field is about  $4/0.2 = 20$  volts/cm at 80 torr, 10 amperes. In these respects, this region resembles the negative glow of a glow discharge which is a region of ionisation and excitation by electrons accelerated in the cathode fall space.

The region of enhanced vapour density necessary for the release of electrons from the cathode may still exist, since the field in the cathode fall space is still high enough to accelerate

the positive ions to sufficient energies to give back-scattering of evaporated atoms. This region of high vapour density would not be detectable at the time-base scanning rates of figs. 24 and 25 since if of the order  $10^{-3}$  cm, this represents one two hundredth of a large division (10  $\mu$ sec.). This should be detectable, but the technique at low pressures was not sufficiently advanced in the present experiments to permit this degree of time scale expansion.

#### 6.7. Thickness of the Cathode Fall Sheath.

In the past, the thickness of the sheaths at the electrodes of an arc discharge have been a matter of conjecture, since unlike the situation in some low pressure discharges these are too small to measure visibly. The method discussed above for measuring the cathode fall and anode fall gives, in principle, a way of measuring the thickness of these sheaths.

In all the oscillograms reproduced so far, the cathode fall is shown as a virtually vertical drop in potential, i.e. the thickness of the sheath is at or beyond the resolution of this method. In most cases the unexpanded time-base speed was about 1 millisecond/cm, the fastest time-base available was 1  $\mu$ sec/cm, so expansion of 1000 times is in theory possible with the present experimental arrangement. Unfortunately, the triggering method was such that beyond scanning rates of 20  $\mu$ sec/cm, the rate of success dropped sharply since the time taken for the anode to reach the cathode was not constant to one part per thousand. Nevertheless, by taking

sufficient oscillograms it was possible to obtain traces at 5  $\mu\text{sec/cm}$  and 1  $\mu\text{sec/cm}$  but the latter was rather faint due to lack of brightness on the oscilloscope screen, fig.31. The anode speed was 40 cm/sec, i.e.  $4 \times 10^{-5}$  cm/ $\mu\text{sec}$ . The cathode fall thickness was, at most 0.1 $\mu\text{sec}$  wide =  $4 \times 10^{-6}$  cm.

#### 6.8. Discussion of Results.

In discussion of their excitation theory of the vapour arc cathode, von Engel and Robson<sup>14</sup> find it convenient to divide the space immediately in front of the cathode into three regions. Region 1, adjacent to the cathode surface, is the fall space in which electrons emitted from the cathode are accelerated. It is a region of high field and high vapour density, and they estimate the thickness to be about  $3 \times 10^{-6}$  cm. In region 2, adjacent to region 1, the electrons have gained sufficient energy in the cathode fall to ionise and excite vapour atoms. Since the electrons are slowed down by these inelastic collisions, the positive space charge is partially neutralised and the field here is much less than in the cathode fall space, region 1. Owing to the low field, the positive ions do not gain sufficient energy to produce significant backscattering and the vapour density falls off by diffusion. Region 2, they estimate has a thickness of about  $10^{-4}$  cm. Region 3, adjacent to region 2, is characterized by a rapid fall in vapour density with distance from the cathode and the transition to electric neutrality which prevails in the column. The true cathode fall is assumed to occur across regions 1 and 2.



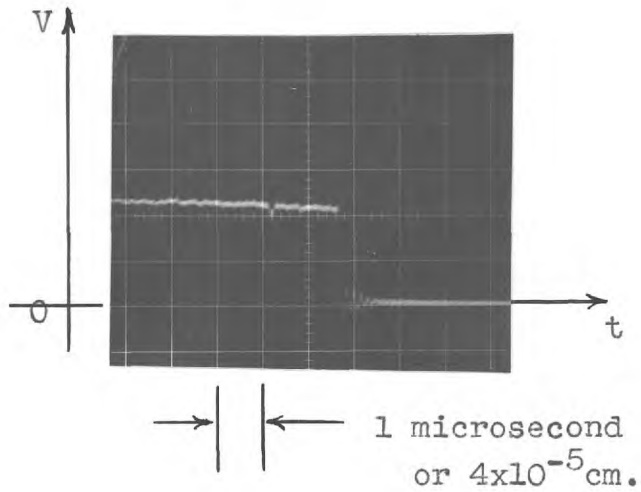


Fig 31. The cathode fall at maximum obtainable resolution.

Tin cathode in argon at 760 torr.  
Graphite anode.

Current: 10 amperes.

Anode B, speed 40 cm/sec, so that  
1 microsecond represents  $4 \times 10^{-5}$  cm.

Scales: V: 5 volt/div  
t: 1 microsec/div.

As the anode approaches the cathode, as was discussed earlier, the anode fall may be expected to disappear when sufficient positive ions are produced there to neutralise the electron space charge. This can be expected to happen when the anode enters region 2, since this is where the ions are produced by electrons accelerated in the cathode fall.

A typical oscillogram is drawn schematically in fig.32, together with the appropriate thicknesses and voltages for a tin cathode in argon at 760 torr. The electric field in the cathode fall space is seen to be at least  $3 \times 10^6$  volts/cm which is insufficient for field emission, and it seems unlikely that the true field is more than ten times this value as required by the field emission theory, fig.2.

In region B, the field is fairly uniform and equal to about  $10^3$  volts/cm. The potential in this region is only slightly above the cathode fall potential, in fact, with poorer resolution this voltage would probably be included in the cathode fall. This is believed to represent a region of enhanced vapour density in front of the cathode where considerable ionisation and excitation take place. Each electron must produce more than one excited atom, since even if electrons are released from the cathode at the rate of one per excited atom, ions must be produced as well either by electron collision with an excited atom, electron collision with an unexcited atom or by collision of two excited atoms. Whichever process operates, the result is similar. The thickness of

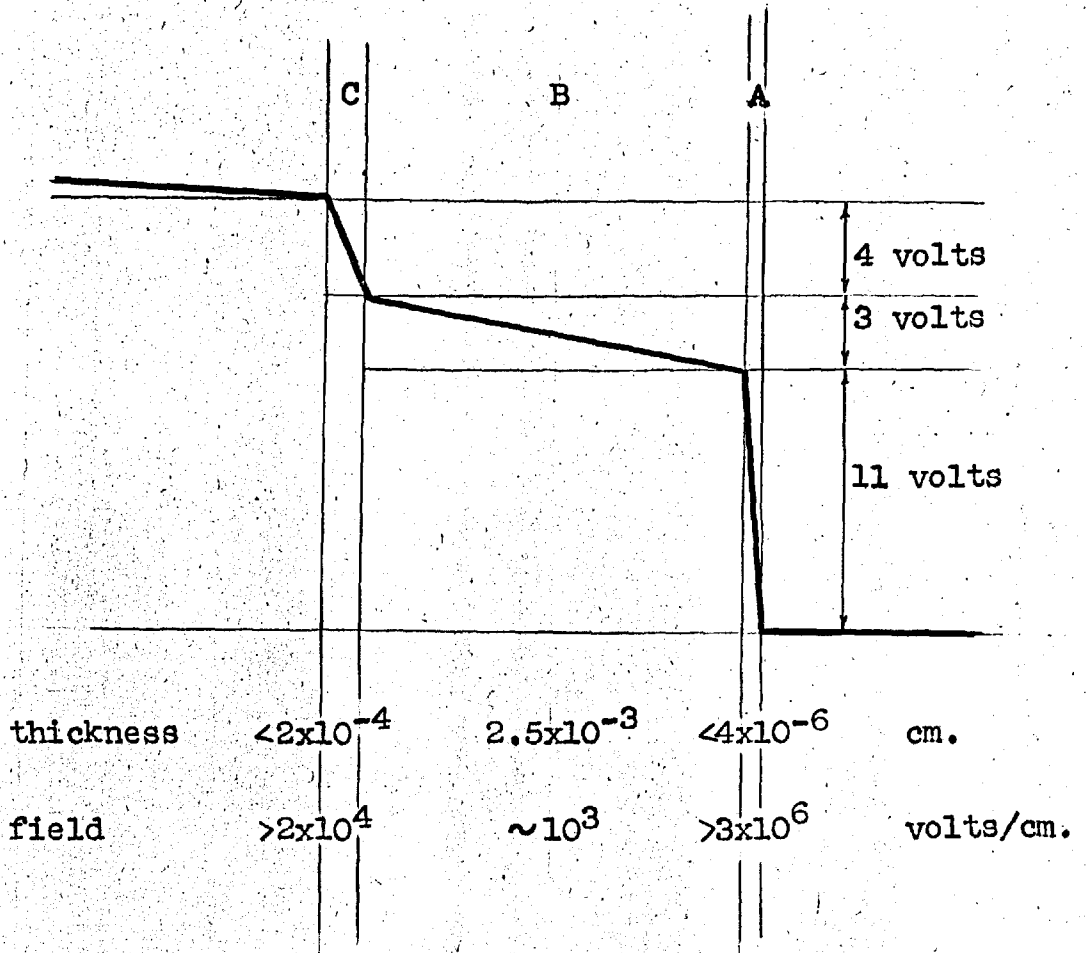


Fig 32 Typical oscillogram.

region B, may thus give an estimate of the size of the mean free path for excitation.

The field in the anode fall space is seen to be at least  $2 \times 10^4$  volts/cm. As was pointed out previously it may be lower than this in some cases, and may even merge with the long column.

CHAPTER VII.      FLUCTUATIONS.

7.1. Introduction.

One of the most characteristic features of the vapour arc are the random voltage fluctuations, of high frequency, clearly visible in the oscillograms, e.g. fig.20. It is seen that the fluctuations are still present after the anode fall has disappeared; this would indicate that they are due to processes at the cathode.

7.2. Experimental Results.

All the experiments described were carried out on a tin dispenser cathode in atmospheric pressure argon, unless otherwise stated. For a 10 ampere arc a typical voltage fluctuation was 0.2 microsecond duration and 0.5 volts amplitude, but superimposed on this was a lower frequency fluctuation of larger amplitude (30  $\mu$ sec, 3 volts). The fluctuations are more marked at low currents. Accordingly a series of electrode drop measurements were carried out at the lowest possible current (3 amperes) to see how the fluctuations changed when the anode fall disappeared.

When the anode fall disappeared, there was a distinct change in the nature and frequency of the fluctuations, fig. 33(a). The amplitude became smaller and the frequency slower. The importance of this observation is that it may enable the thickness of the cathode region to be estimated, even when there is no definite voltage step as the anode fall disappears. An example

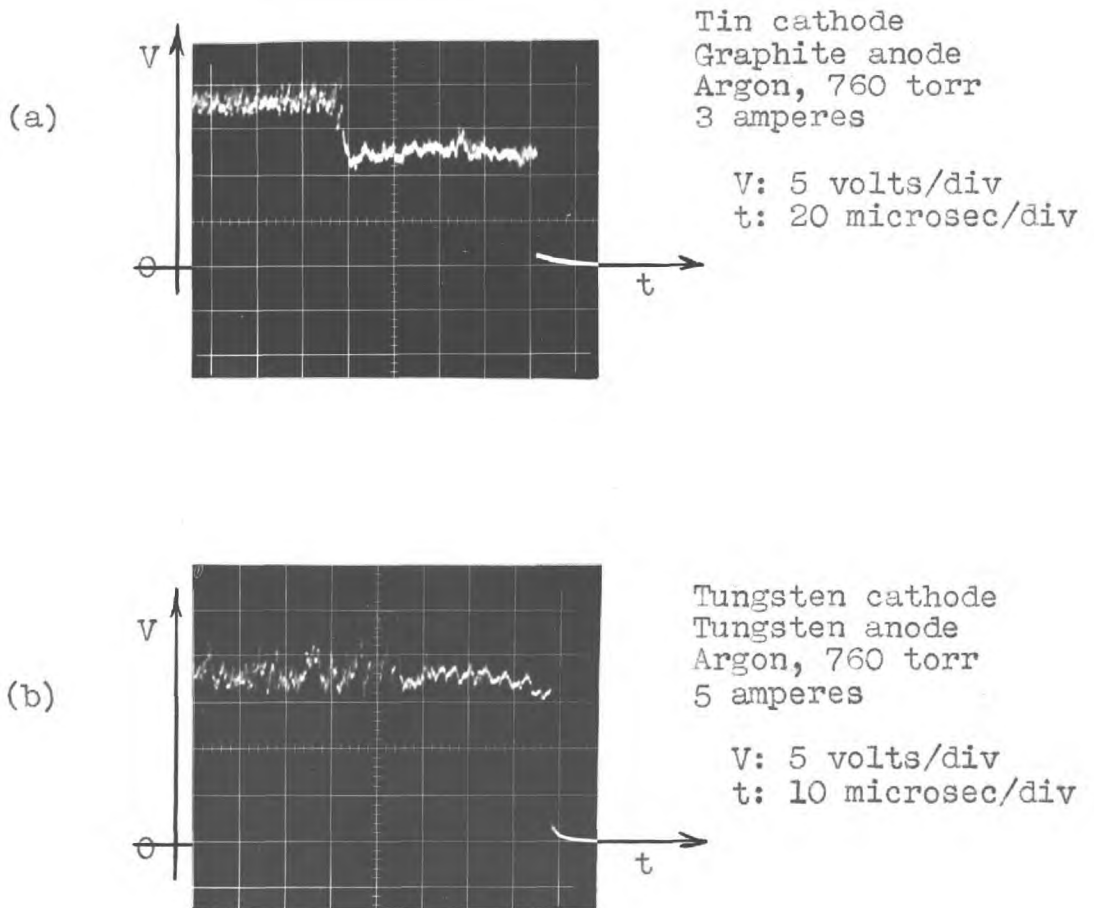


Fig 33. Change in the nature of the fluctuations as the anode fall disappears.

of this is given in (b), the case of tungsten electrodes in argon; the anode fall is marked by a change in slope of the voltage versus gap trace, but on expanding the timescale no further discontinuity is observed - except for this change in the nature of the fluctuations.

In fig.33(b), the length of the cathode region, on the above assumption, is 33 microseconds which represents a thickness of  $1.2 \times 10^{-3}$  cm (anode speed 35 cm/sec), which is the same as for the vapour arcs which gave definite steps (see fig.28).

### 7.3. Discussion.

It has been verified that the cold cathode arc exhibits voltage fluctuations with frequencies greater than  $10^6$  cycles per second, and that their amplitude increase with decreasing current.

It has also been shown that while these are a predominantly cathode phenomenon, there is a contribution from the anode region which is at a higher frequency. The presence of these fluctuations, and their change when the anode fall disappears enables the cathode fall thickness to be estimated when this is not possible by other methods.

The fluctuations have been attributed to the increased recombination surface afforded by droplets of material ejected from the cathode<sup>46</sup>; other workers<sup>47</sup> prefer to explain it by the inherent instability of a process which depends on ions which have at least two roles, supplying energy for evaporation and directly or indirectly causing electron emission. There is insufficient data in the present experiments to add to these opinions.

CHAPTER VIII.      CONCLUSIONS.

8.1. The Tin Dispenser Cathode.

This form of cathode has certain advantages which may justify its use in certain practical applications. The ejection of large droplets of cathode material is much reduced compared with a pool cathode, and the cathode still has the outstanding advantage of the liquid cathode - that the surface is reformed if damaged. In addition, the cathode spot movement is less erratic than on many other cold cathodes; it is this factor which led to the success of the present series of measurements.

At the moment, the usefulness of the cathode is somewhat limited owing to the lack of a suitable porous refractory metal. Presumably this could be solved in time, but it was not thought wise in the present work to devote too much time to this aspect of the device.

To a certain extent the cathode would have to be matched to a certain current so that the porosity of the porous metal could be chosen accordingly, unless some sort of variable speed pump could be contrived to control the feed rate of tin.

The cathode is applicable at any orientation, provided suitable arrangements are made for the tin feed.

It has been established that the cathode voltage drop is the same irrespective of the form of the cathode, being a function only of the cathode material. The cathode fall for tin is not



particularly low, but rough experiments have indicated that the cathode fall could probably be lowered considerably by the addition of alkali metals in small proportions to the tin. This technique has been successfully used by Reiling<sup>48</sup> on mercury cathodes.

### 8.2. A New Method of Separating the Cathode Fall from the Anode Fall.

By means of a new technique it has proved possible to measure separately the cathode fall and anode fall of a high pressure arc discharge. This represents a significant advance in arc measurement technique.

Attempts to use probes have been tried in the past and in the present work, but they are doomed to failure owing to the disturbance caused in a high pressure discharge, and by the number of uncertainties in the interpretation of the results. Also, probes can never hope to measure the fine structure of the electrode regions.

The method has been successfully applied to cold or vapour arc cathodes, results on thermionic cathodes are less successful; this may be due to the lack of a dense vapour region in front of the latter.

The method permits the potential distribution in the region of dense vapour in front of the cathode to be deduced, and the thickness of this region to be estimated.

### 8.3. Thickness of the Fall Sheaths.

In principle, the method permits measurement of the thickness of the fall sheaths in front of the cathode and anode. In practice,

owing to shortcomings of the present technique, it has been possible to put maximum values only to these distances. Nevertheless, the results are valuable.

#### 8.4. Suggestions for Future Work.

The work described in this thesis on the separate measurement of the cathode fall and anode fall of an arc discharge must surely represent only the beginning of a new era in arc measurements since it offers not only a method of measuring these potential falls, but also the possibility of deducing complete potential distributions in the electrode regions. There follows now suggestions for further work using this method.

##### (1) Thickness of the Fall Sheaths.

At first sight this seems to imply simply the use of a faster oscilloscope, or a much slower rate of approach. It may be possible to use a slower rate of approach, in this work only a convenient value was used not an optimum, but it is doubtful whether more than a factor of ten could be gained this way. In order to use a faster oscilloscope a far better method of triggering the sweep would have to be found. This may require an entire rethinking of the present method.

##### (2) The Mercury Arc.

Since so much is known about the mercury arc, it would be very interesting indeed to carry out this type of measurement on a mercury cathode.

REFERENCES:

1. Petroff, W. (1803), Rep. Acad. Chirurg. Med. Petersburg.
2. Davy, H. (1812), Elements of Chemical Philosophy, 1, 152.
3. Ayrton, H. (1910), The Electric Arc.
4. von Engel, A. and Steenbeck, M. (1934) Elektrische Gasentladungen.
5. Grotian, W. (1915), Ann. d. Physik, 47, 141.
6. Mitkewicz, W. (1903), Z. russ. Phys. Ges. 35, 507, 675.
7. Stark, J. (1904), Phys. Z. 5, 750.
8. Suits, C.G. (1935), Physics 6, 190, 315.
9. von Engel, A. and Steenbeck, M. (1931), Wiss. Veroff. Siemens, 10, 155.
10. Edels, H. and Whittaker, D. (1957) Proc. Roy. Soc. A, 240, 54.
11. Froome, K.D. (1949) Proc. Phys. Soc. 62B, 805.
12. Suits, C.G. (1939), Phys. Rev. 55, 561.
13. von Engel, A. and Robson A.E. (1957) Proc. Roy. Soc. A, 242, 217.
14. von Engel, A. (1965) Ionised Gases, 2nd Edition.
15. Slepian, J. (1926), Phys. Rev. 27, 407.
16. Weizel, W., Rompe, R. and Schon, M. (1950) Z. Phys. 115, 179.
17. Smith, C.G. (1942), Phys. Rev. 62, 48.
18. Rothstein, J. (1950), Phys. Rev. 78, 331.
19. Gomer, R. (1961), Field Emission and Field Ionisation.
20. Langmuir, I. (1923), G.E. Review, 26, 735.
21. Mackeown, S.S. (1929), Phys. Rev. 34, 611.
22. Fowler, R.H. and Nordheim, L.W. (1928), Proc. Roy. Soc. A119, 173.

23. Hull, A.W. (1962) Phys.Rev. 126, 1603.
24. Gabor, D. (1963) Advanced Energy Conversion, 3, 307.
25. Massey, H.S.W. (1930) Proc.Camb.Phil.Soc. 26, 387.  
Cobas, A. and Lamb, W.E. (1944) Phys.Rev., 65, 327.
26. Oliphant, M.L.E. (1929) Proc.Roy.Soc. A.124, 228.  
Dorrestein, R. (1942) Physica, 9, 433.
27. Tonks, L. (1936), U.S.Patent 2128861.
28. Steenbeck, M. and Berthold, R. (1936) Deutsches Reichpatentschrift  
638208.
29. Hewitt, P.C. (1912), U.S. Patent 22246.  
Weintraub, E. (1905), Trans.Amer.Electrochem.Soc. 7, 273.
30. Tonks, L. (1938) Phys.Rev. 34, 634.
31. Edels, H. (1961) Proc.I.E.E. 108A, 55.
32. Loeb, L.B. (1939) Fundamental Processes of Electric Discharges  
in Gases, 274.
33. Langmuir, I. and Mott-Smith, H. (1924), G.E.Review, 27, 539.
34. Nottingham, W.B. (1928), J.Franklin Inst. 206, 43.
35. Bramhall, E.H. (1932), Phil.Mag. 13, 682.
36. Mason, R.C. (1932), Phys.Rev. 40, 1045.
37. Mason, R.C. (1937), Phys.Rev. 51, 28.
38. Cozens, J.R. and von Engel, A. (1965) Int.J.Electronics, 19, 61.
39. Francis, G. (1956) Handbuch der Physik, 22, p.83.
40. von Engel, A. and Arnold, K.W. (1962) Proc.Phys.Soc. 79, 1098.
41. Mitchell, A.C.G. and Zemansky, M.W. (1934) Resonance Radiation.
42. Bauer, A. and Schulz, P. (1954) Z.Phys. 139, 197.
43. von Engel, A. and Arnold, K.W. (1960, Nature, 187, 1101.

44. Robson, A.E. (1955) E.R.A. Report L/T340.
45. Froome, K.D. (1950) Proc. Phys. Soc. 63B, 377.
46. von Engel, A. Private communication.
47. Keseav, I.G. (1964) Cathode Processes in the Mercury Arc.
48. Reiling, G.H. (1962), I.R.E. Trans. ED-9(3), 271.